

Article

# Timing of Opalization at Lightning Ridge, Australia: New Evidence from Opalized Fossils

George E. Mustoe <sup>1,\*</sup>  and Elizabeth T. Smith <sup>2</sup><sup>1</sup> Geology Department, Western Washington University, Bellingham, WA 98225, USA<sup>2</sup> Australian Opal Centre, P.O. Box 229, Lightning Ridge, NSW, Australia; elizabethtsmith@exemail.com.au

\* Correspondence: mustoeg@wwu.edu

**Abstract:** Microscopic analysis of fossils from the Lightning Ridge district of northwestern New South Wales, Australia, shows that opal has been typically deposited in variable cavities left by the degradation of the original organic material. Fine-grained, clay-rich sediments have preserved the external morphology, and opalization has produced detailed casts with different modes of preservation of internal details. Plant remains include cones, cone scales, fruiting bodies, and seeds, but the most common specimens are twigs, stems, and wood fragments. These specimens commonly contain angular inclusions that represent small tissue fragments produced by the degradation of the original wood. Inclusions commonly have a “hollow box” structure where the organic material has decomposed after the initial opal filling of the mold. These spaces commonly contain traces of the cellular architecture, in the form of wood fiber textures imprinted on the cavity wall, degraded cellular material, and silicified tracheids. Opal casts of mollusk shells and crustacean bioliths preserve the shape but no calcium carbonate residue. Likewise, opal casts of vertebrate remains (bones, teeth, osteoderms) lack preservation of the original bioapatite. These compositions are evidence that burial in fine clays and silts, isolated from the effects of water and oxygen, caused protracted delays between the timing of burial, decomposition, and the development of vacuities in the claystones that became sites for opal precipitation. The length of time required for the dissolution of cellulosic/ligninitic plant remains, calcium carbonate items, and calcium phosphates in bones and teeth cannot be quantified, but evidence from opal-bearing formations worldwide reveals that these processes can be very slow. The timing of opalization can be inferred from previous studies that concluded that Cenozoic tectonism produced faults and fissures that allowed horizontal and lateral movement of silica-bearing groundwater. Comparisons of Australian opal-AG with opal from international localities suggest that opalization was a Neogene phenomenon. The transformation of Opal-AG → Opal-CT is well-documented for the diagenesis of siliceous biogenic sediments and siliceous sinter from geothermal areas. Likewise, precious and common opal from the late Miocene Virgin Valley Formation in northern Nevada, USA, shows the rapidity of the Opal-AG → Opal-CT transformation. Taken together, we consider this evidence to indicate a Neogene age for Lightning Ridge opalization and by inference for the opalization of the extensive opal deposits of the Great Artesian Basin in Australia. New paleontology discoveries include a surprising level of cellular detail in plant fossils, the preservation of individual tracheids as opal casts, evidence of opalized plant pith or vascular tissue (non-gymnosperm), and the first report of Early Cretaceous coprolites from New South Wales, Australia.



**Citation:** Mustoe, G.E.; Smith, E.T. Timing of Opalization at Lightning Ridge, Australia: New Evidence from Opalized Fossils. *Minerals* **2023**, *13*, 1471. <https://doi.org/10.3390/min13121471>

Academic Editor: Olev Vinn

Received: 26 October 2023

Revised: 20 November 2023

Accepted: 21 November 2023

Published: 23 November 2023



**Copyright:** © 2023 by the authors. Licensee MDPI, Basel, Switzerland. This article is an open access article distributed under the terms and conditions of the Creative Commons Attribution (CC BY) license (<https://creativecommons.org/licenses/by/4.0/>).

**Keywords:** Australia; fossilization; Lightning Ridge; opal; paleontology

## 1. Introduction

Opalized wood is known from the opal deposits of North America and Ethiopia [1,2], but apart from two or three insects in opal from Java [3] and a few opalized gastropods from Indonesia [4], opalized invertebrate and vertebrate remains are exclusively an Australian product. Apart from their aesthetic appeal, fossils provide vital information on

age dating for the Great Artesian Basin (GAB) and other Australian Cretaceous deposits, for paleoenvironment and paleoclimate reconstruction, the determination of evolutionary relationships, and paleobiogeography.

The current formation models for opal in the GAB focus entirely on the development of commercial opal in seam (veins) and nobby (nodular) forms. They do not address fossil formation, although fossils are a significant source of commercial opal. In many sites, fossils are the major component of opalized materials and the largest opalized objects in the strata. Unlike opal in seams and nobbies, the fossils can be regarded as “primary structures” because their taphonomic placement and the biominerals they contributed were present at deposition.

The purpose of this study was to gain novel insights into aspects of mineralogy, preservation modes, and the diagenesis of the diverse and abundant opalized fossils from the Lightning Ridge fields.

The theories on the origin and timing of sedimentary opalization in Australia are marked by diversity, uncertainty, and disagreement. Did opal formation occur in the Late Cretaceous, mid-Cenozoic, or in the Recent era? Was it shortly after deposition or during the time when the original volcaniclastic sediments were being diagenetically transformed to claystone, or were secondary end-product clays the key to chemical reactions that caused the precipitation of opal microspheres? Was silica-bearing groundwater produced from the acidic oxidative weathering of sandy sediments overlying the opal-bearing claystone or was silica introduced from below by the upwelling of artesian water? Were ancient or modern microbes essential participants in opalization? The various hypotheses (summarized below) that have been advanced to explain Lightning Ridge opal genesis have included all these factors.

The goal of our research was not to resolve the discrepancies in formation theories. However, during our investigations, we found unexpected evidence relevant to the timing of opalization, providing useful constraints for evaluating the different models.

In the course of this work, we examined other lines of evidence from locations outside Australia. These provide information about the diagenetic relationships of opal-AG and opal-CT based on occurrences of biogenic siliceous sediments and in siliceous, hot-spring sinter. We also discuss the occurrence of opal in Nevada, USA, focusing on the Miocene deposits of Virgin Valley, where precious opal has been mined for more than a century.

The combined paleontological and geological evidence supports the interpretation that the opalization of the Early–mid Cretaceous sediments of the Australian opal fields occurred principally in the Neogene.

## 2. Geological Setting

Commercial opal deposits in Australia are mostly located within the Great Artesian Basin (GAB), where a large inland sea existed during the Early Cretaceous (Figure 1). The GAB contains extensive Mesozoic strata, with a total area of 173,500 km<sup>2</sup> and an average depth of ~500 m [5,6]. The GAB records the transgression and regression of the epicontinental Eromanga Sea. The Eromanga and Surat Basins occupy most of Queensland, northwestern New South Wales, and part of northeast South Australia (Figure 1). These basins developed in association with the Cordillera Orogen, acting as depocenters for the Whitsunday Volcanic Province, “the largest known silicic-dominated volcanic province in the world” [7], deposited over 4050 Ma during the Early–mid Cretaceous.

The Eromanga Sea was shallow, poorly connected to the open ocean, muddy, stagnant, and anoxic in parts [8]; it receded from Lightning Ridge earlier than from the adjoining Eromanga Basin, before deposition of the opal-bearing sediments. Marine sequences were replaced by thick continental sandstones and claystones of the Rolling Downs Group, which includes outcrops of the Griman Creek Formation (GFC) between the townships of Lightning Ridge (NSW) and Surat (QLD) [9].

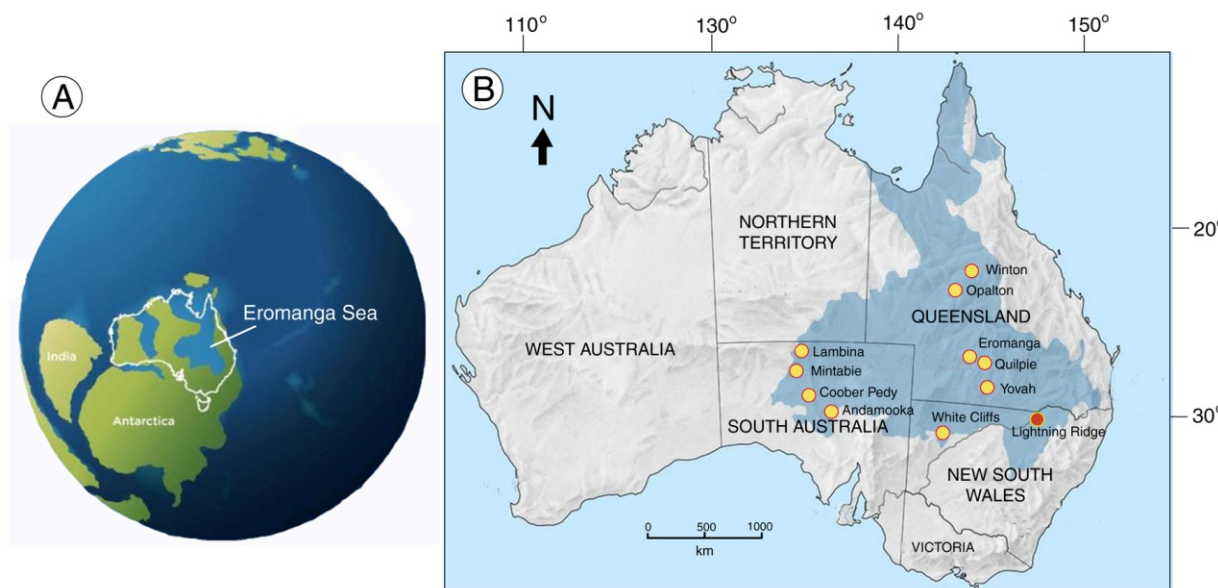


**Figure 1.** Location map. (A) Global view showing Gondwana continental land masses in the Early Cretaceous, when inland seas occupied much of central Australia. (B) Strata of the Great Artesian Basin are shown in blue. Yellow circles indicate the locations of the major opal mining districts. Lightning Ridge is shown in red.

Up to 400 m thick, the GFC includes the Wallangulla Sandstone and Coocoran Claystone members that host the opal-bearing strata near Lightning Ridge (Figure 2). The GFC tracks the transition from marine and near-shore environments to a mosaic of permanent and seasonal freshwater systems and active alluvial/fluviatile settings.

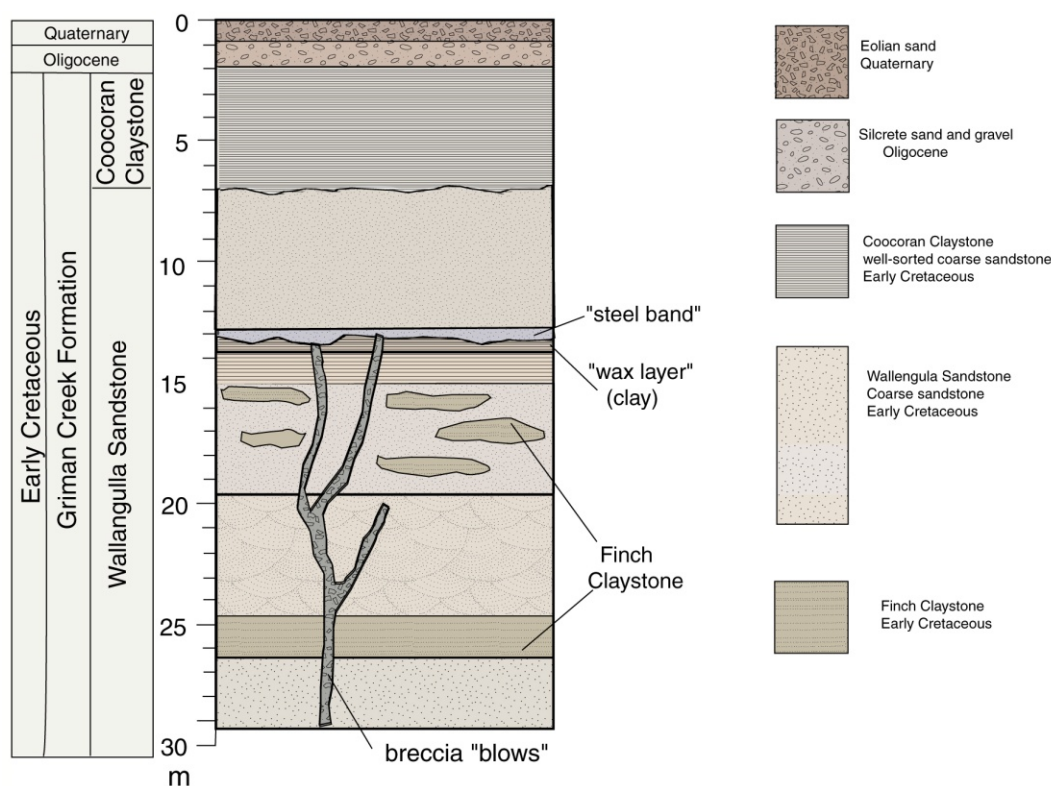


**Figure 2.** Generalized stratigraphy at Lightning Ridge, adapted from [10].

In the opal fields, opalized fossils, commercial opal, and potch (“common” opal) are found in the fine-grained Finch Claystone facies (“opal dirt”) within the Wallangulla Sandstone. These thin claystone lenses represent freshwater channel deposits in sandstone that is marked by cross-bedding, rip-up clasts, bioturbation, and fining-upward sequences [9,10]. The Finch Claystone lenses are laterally discontinuous and occur to depths of 30 m or more beneath the ground surface, with the two main opal- and fossil-producing levels at 12–15 m and at 25–30 m. Local stratigraphy is poorly resolved.

Commercial opal-AG or  $\text{SiO}_2 \cdot n\text{H}_2\text{O}$  (hydrated silicon dioxide) is often found at a slight nonconformity, overlain by a harder “steel band”, which is a distinctive, indurated siliceous layer with large quartz grains and quartz-mineralized wood, inferring more active fluvial conditions.

Opal-bearing sediments at Lightning Ridge are rich in volcanioclastic material. In some areas, the paleochannels are directly below a well-defined layer of extremely fine smectite/bentonite clay known as a “waxy band”, evidence of a major ashfall event or events dated by U/Pb as 100.2–96.6 Ma [10,11]. The Finch Claystone is therefore best described as mid-Cretaceous (Cenomanian). Finch Claystone “opal dirt” includes fine silt, clays, and older reworked ash layers, and is characterized by its malleability and hydroplasticity. The material expands massively when wet and shrinks and fractures heavily on desiccation. The sedimentary rock is variable and inconsistently loaded with opalized organic matter and potch and precious opal in nodular (nobby) and seam (vein) form.

The geology of the Lightning Ridge area has been described in detail by many investigators; comprehensive overviews and bibliographies were published by [8,12]. However, we provide the first in-depth report on the fossil mineralization.

### 3. Site History

Opal mining began circa 1887 with the discovery of “black” opal on the low ridges known as Wallangulla, north of Walgett, along the old stock route to Queensland. By 1903, hundreds of hand-dug shafts had been sunk; mining extended over a wide area and the town of Lightning Ridge was surveyed. During those first decades, mining was done by candle- or lamplight, with pick and shovel, wheelbarrow, and windlass. The slow pace of activity increased in the 1960s when new machinery was introduced for reprocessing old surface mullock and for the extraction and processing of the opal clays. From those early days, Lightning Ridge has been famous as the world’s principal source of precious black opal [13], but the locality is also unique in producing opal types typical of other GAB fields, i.e., “crystal” (translucent), white, gray, and “matrix” opal, and black opal, unique gemstones in which precious opal of unequalled pattern and brilliance superimposed against an inky, black background of common opal.

Over time, prospecting and excavation principles have remained unchanged and opal mining is basically a small-scale, localized, non-corporate activity. Portable drill rigs are now used to locate the opal-bearing claystone below optimal red sandstone. Shafts are sunk to allow the mechanical excavation of opal-bearing rock that is subject to machine washing to reveal the small amounts of precious opal.

Mining methods are integral to on-field paleontology, creating collection biases, and destroying taphonomic information and fine-scale stratigraphy. Fossils are seldom observed in situ and are instead found in “tailings”, the residue from machine washing which breaks up articulated and associated specimens, reduces scientific information, and causes surface abrasion that destroys fine projections and textures on fossil specimens. On the positive side, mining is essential for fossil recovery, and the large volume of processed sediment from widely dispersed sites has enabled fossil sampling over a huge area. Disjunct opal mining activity now extends over 2000 km<sup>2</sup> in the Lightning Ridge region, with much prospective ground that is still unexplored and untested.

#### 4. Opal Nomenclature

Two basic systems are used to categorize opals. One system is based on gemological properties, established by Australian gemstone trade organizations [14]. This classification divides natural opal into precious opal, which exhibits “play of color” (POC) caused by the diffraction of white light by the orderly microstructure, and common opal or potch, which is opal that has a disorderly arrangement of silica microspheres and hence an absence of play of color. These natural opals are subdivided into three types determined by their relationship to the background host rock: “all opal”, “boulder opal”, and “matrix opal”. A standard chart using numbers N1 to N9 is used by gemologists to assess and describe the darkness or lightness of the body tone in precious opal. Informally, opal is sometimes described as “light”, “medium”, or “dark”. “Black opal” is a term used for precious opal that overlies or is intermixed with black potch, providing a dark base color. Gemology nomenclature also includes categories for natural opal that has been treated artificially in various ways and for synthetic and artificial opal. These terms are useful for grading gems, but they are sometimes used to describe opal samples used in scientific investigations, particularly in Australia.

The second classification is based on mineralogy and microarchitecture. This nomenclature followed the realization in the 1930s that opal occurred both in amorphous forms and in forms that had incipient crystallinity [15,16]. The nomenclature was formalized by Jones and Segnit [17,18]. They divided natural opal into Opal-A (nearly amorphous  $\text{SiO}_2$ ), Opal-C (well-ordered  $\alpha$ -cristobalite), and Opal-CT (disordered  $\alpha$ -cristobalite and  $\alpha$ -tridymite). This nomenclature has been modified to divide Opal-A into subdivisions [19]. Amorphous varieties composed of microspheres are now often designated as Opal-AG. This classification system was expanded to include Opal-AN, an anhydrous glassy form of  $\text{SiO}_2$  (hyalite) that is produced in volcanic environments [20]. There is not yet an Opal-A subdivision defined for biogenic opal of the type secreted by diatoms, radiolarians, and sponges, where amorphous silica lacks microsphere architecture [21].

Because we describe an Australian locality, we follow the national convention of using Opal-AG in preference to Opal-A. Among gemologists, “common opal” and “potch” are often used interchangeably to describe opal without play of color. Potch and precious opal both consist of amorphous opal, the difference being the uniform size and regular lattice arrangement of microspheres in the latter. In contrast, the term “common opal” has long been used by geologists and amateur collectors to describe forms of silica that have incipient crystallinity (e.g., Opal-CT). In this paper, we avoid using the term “common opal” and instead describe non-precious opal as potch. One nomenclatural caveat: the terms Opal-AN and Opal-AN have been used interchangeably; Opal-AG and Opal-AG are equivalent.

Nomenclature related to the genesis of opal is variable. We use “opalization” to refer to the formation of any opal, regardless of the specific mineralogic form or the regional extent of the deposit. In the Great Artesian Basin of Australia, silicification has occurred over a vast area, with the greatest volume involving the siliceous cementation of porous sediments, producing silcretes across the entire GAB and “shincracker” (heavily silicified sandstones and porcellanite) and “steel band” at Lightning Ridge. In productive strata, the volume of “potch” greatly exceeds the relatively tiny amount of precious opal. The distribution of play-of-color (POC) opal is patchy, limited, and unpredictable. Our research focuses on opalized fossils from the Finch Claystone and adjoining “steel band” because the silcrete and sandstone layers at Lightning Ridge generally do not contain fossils or opal.

#### 5. Opal Formation Hypotheses

##### 5.1. Deep Weathering

This hypothesis has a long history, including Rey’s [8] important theory of oxidative weathering. Various interpretations were presented in detail by Hermann and Maas [11], who placed opalization at around 29 Ma. The formation of sedimentary Opal-AG was

the result of the intensive weathering of Cretaceous host rock. Shuttle Radar Topography Mission (SRTM) images reveal ancient river channels of a deltaic system, now represented by pedogenic silcrete that caps opal-bearing sediments in the Lightning Ridge district. The rivers provided an intermittent source of water that resulted in localized deep weathering and silicification in reactive volcaniclastic sediments. Wet/dry cycles controlled eH and pH, converting detrital feldspar to kaolinite, accompanied by the release of silica, accompanied in turn by the formation of opal spheres. Opalization occurred during the initial phase of acidic oxidative weathering at the redox front near the surface, where reduced lithologies and groundwater met oxic conditions. Subsequent, less-intense weathering under oxidizing conditions modified the weathering profiles but produced little additional opal.

### 5.2. Syntectonic Opalization

The depositional model proposed by Pecover [22–29] relied on studies of opal seam deposits that occur in horizontal and vertical zones of intense brittle fracture deformation. Seams or veins of opal are inferred to have formed rapidly via a process of faulting and fracture of host rock during the Cenozoic deformation of Cretaceous sandstones and claystones. The polymerization of dissolved silica produced viscous fluids propelled by seismic-fluid pumping and hydraulic extension fracturing. Seam arrays are dominated by potch with internal textures suggesting multiple episodes of viscous opal flow into cracks and fractures in host claystones. The model relies on the transport of basinal fluids in vertical “blows”, which are columns of brecciation that extend between adjacent strata. Precious opal is confined to areas where arrested fluid flow allowed the development of colloidal photonic lattices. Soluble silica is inferred to have come from sediment dewatering and the leaching of silica from siliceous plant phytoliths. Cross-cutting vein or seam geometries are evidence of multiple episodes of silica precipitation. This opalization is interpreted as being associated with plate-tectonic compressive events during the Miocene.

### 5.3. Cretaceous Microbial Origin

A very different explanation for opalization is that Cretaceous microbes produced organic and carbonic acids that aided the biochemical weathering of clay minerals and feldspar to release soluble silica. [30–32]. The environment required for microbial growth is inferred to have resulted in opal precipitation over a few months, not the hundreds of thousands of years envisaged by the deep weathering model. Instead, opal formed as part of the diagenetic process during the Early Cretaceous in near-surface aerobic environments at temperatures of <35 °C and at near-neutral pH.

Herrmann et al. [33] observed that organic carbon and metallic sulfides are the cause of dark pigmentation in Lightning Ridge black opal. They concluded that these pigments were the result of sulfate-reducing bacteria that lived at the time when opal was being precipitated, a process that ceased with a shift from reducing to more oxidizing conditions following the arrival of a weathering front.

### 5.4. Modern Microbial Origin

The radiocarbon dating of carbon extracted from black potch has yielded ages of 7000–1000 Cal BP. Deuterium,  $^{18}\text{O}$ , and  $^{13}\text{C}$  suggest that opalization was a modern phenomenon [34]. Deveson [35] cultured four types of microbes from locations near Lightning Ridge, including a red fluorescent form that was proposed as evidence of a very young age for opalization.

### 5.5. Artesian Water/Mound Springs Model

The Lightning Ridge opal field lies on a line of natural artesian springs (“mound springs”) which have been active since the late Pleistocene. The formation of amorphous silica spheres is assumed to have resulted from a combination of cooling temperature, pH

change, and the presence of pre-existing nuclei [36–38]. According to this model, clay minerals in the claystone host matrix allowed cation-exchange reactions that released hydrogen to neutralize alkaline groundwater and absorb ionic impurities that interfered with silica precipitation. Fracture networks were formed by hydraulic pressure when the clay layer acted as an impermeable and flexible membrane. Like the syntectonic model, this hypothesis assumes the movement of hydrothermal fluids through vertical brecciation columns (“blows”).

The involvement of artesian water in opal formation is supported by the work of Dickson [39], who observed that Lightning Ridge opals contain anomalous levels of Eu relative to Sm and Dy. The opal host rocks do not show this anomaly, suggesting that the bedrock sources of dissolved silica were external to opal-bearing layers. Calcite cements within rocks hosting the aquifers of the Great Artesian Basin have positive Eu anomalies, suggesting that opal was formed by the upwelling of artesian waters.

### 5.6. Gamma Radioactivity and Nano-Nuclides

Gamma-ray radioactive logging demonstrates natural radioactivity surrounding opal deposits, increasing in intensity towards the central precious opal zone. Neutron activation analysis and secondary ion spectroscopy (SIMS) of precious opal reveal thorium, uranium, lead, and anomalous concentrations of daughter nuclides produced by natural uranium fission. This suggests the possibility that silica spheres in precious opal formed around a radioactive nano-nucleus of a heavy-atom compound that produced catalytic heterogeneous nucleation and growth. Microspherulite superlattice arrangements developed in silica-bearing groundwater, prior to ordered sedimentary packing and settling [40].

### 5.7. Rapid Opal Synthesis

Successful attempts to reproduce the synthesis of opal with an orderly molecular arrangement sufficient to produce play of color date back to 1967, when Pierre Gilson produced synthetic opal with water content similar to that of natural opals. His work was preceded by techniques developed by the Australian CSIRO (Commonwealth Scientific and Industrial Research Organization) and patented in Australia, Great Britain, and the USA in 1964 [41]. The problem with synthetic opals as an analog for natural opal is the lack of silica in the spaces between silica spheres in the synthetic versions. Several strategies have been invented to address this problem. The original Gilson process was adapted to introduce small zirconium-oxide spheres in combination with the larger silica spheres. In 1980, the Gilson patents and processes were sold to Kyocera, a Japanese company. Synthetic opals presently being marketed commonly contain plastic resin as a filler material, allowing the production of gemstones that have a rainbow of body colors. Despite their gemological qualities, the synthetic genesis of these opals has little relevance to the origin of natural opal.

A second line of evidence derives from attempts to produce precious opal using naturally-sourced local materials, the best known of which is the work of Lightning Ridge opal miner, Len Cram [42,43]. A self-taught chemist and mineralogist, Mr. Cram aimed to prove that the sedimentary deposits of the Great Artesian Basin are evidence of the Biblical Great Flood [44,45]. He began by mixing various combinations of ingredients to precipitate opal and demonstrated that opal can develop rapidly, requiring an electrolyte solution, a source of dissolved silica, and some alumina and feldspar. The basic ingredient in his recipe is tetraethylorthosilicate (TEOS), an organic molecule containing silica (which incidentally is neither naturally-sourced nor local). The high concentration of dissolved Si in TEOS favors rapid opal precipitation; the amount of alumina determines the hardness. The opal-forming process is one of ion exchange, a chemical process that involves building the opal structure ion by ion. Details of the process remain confidential, but [46] provides an overview. As with the Gilson and Kyocera synthetic opals, the difficulty is converting the soft precursor opal into a hardened product equivalent to natural opal. Cram and Shepherd maintain that their experiments

confirm that Lightning Ridge and other Australian opal fields were generated in modern times, consistent with the creationist view that Earth is only 6000 years old.

## 6. Opal Topologies

Opal occurs at Lightning Ridge in a variety of topologies or forms. These include seam opal, nobbies, septarian and reticulated networks, “ball-and-pillow” structures, and opalized fossils. Each of these forms can consist of potch, precious opal, or an intermixture of both opal types. Opal also occurs as sedimentary cement in clastic host rock, the “steel band” zone.

### 6.1. Seam Opal

“Seam opal” fills small fractures or veins in the host claystone (Figure 3), in some cases showing complex cross-cutting relationships that are evidence of multiple episodes of opal deposition, as discussed in detail by Pecover [28]. In opal fields west of Lightning Ridge (e.g., Grawin, Glengarry, and Sheepyard), opal commonly occurs in seam form, locally in large flat slabs and “plates”.

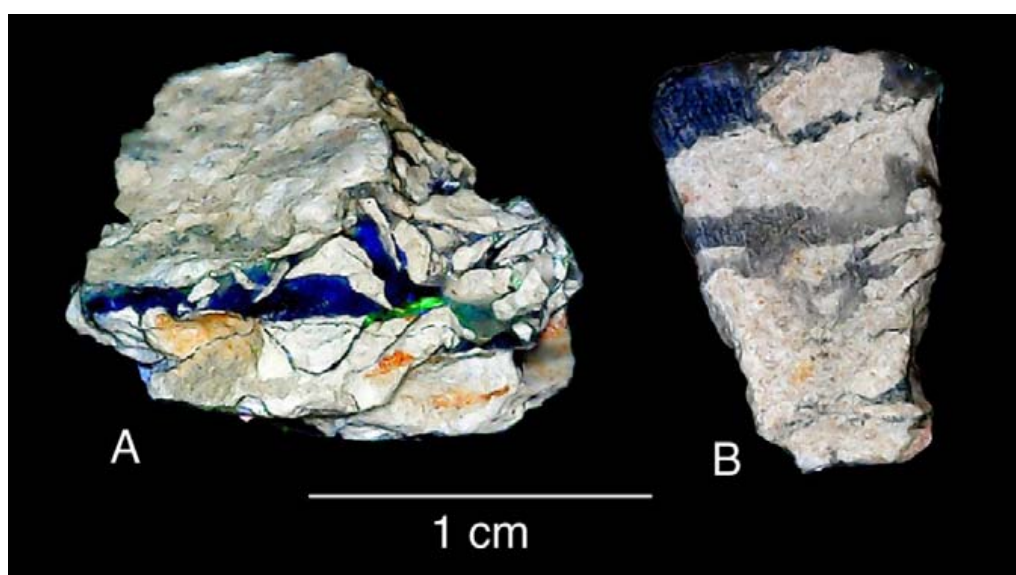


**Figure 3.** Reflected light views of claystone containing precious opal and potch in seams that fill fracture networks. (A) Geometrically complex seams of precious opal in highly fractured claystone, Specimen GM-100. (B) Precious opal and potch in subparallel fractures, Specimen GM-101.

### 6.2. Nobbies (Nodules)

The second major form of opal consists of opal in lumps and masses that show no obvious pathways for the entry of silica. These are referred to as “nobbies” (Figure 4). Nobby topologies are highly variable: amorphous, rounded or flat, commonly with conical caps and distinctive radiating ridges. Nobbies are restricted to the Lightning Ridge opal fields, found nowhere else on Earth. Although they are the primary source of precious black opal, the vast majority of nobbies contain only potch. Like seam opal, nobbies are secondary structures, derived from silica infill at weak points or openings in the claystone. Their origin has received much attention from researchers over many years; Herrmann and Maas [12] provided an authoritative analysis.

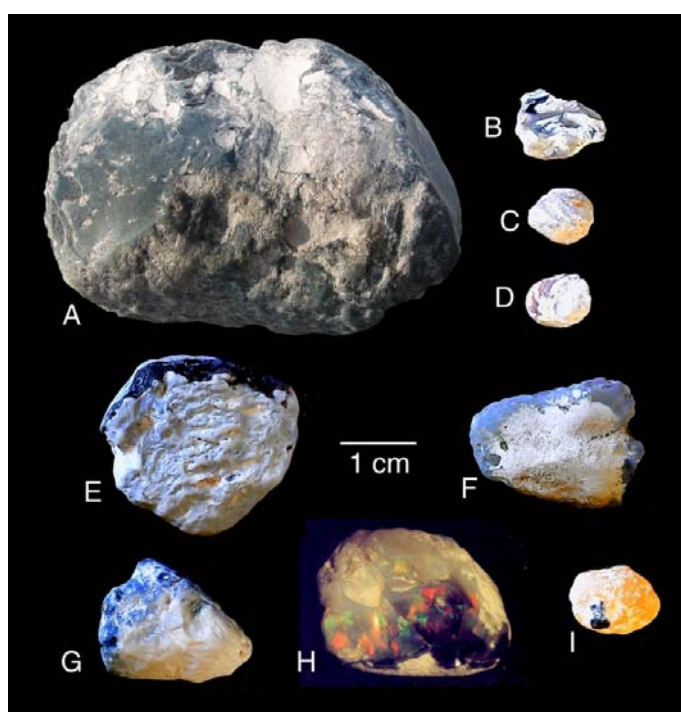


**Figure 4.** Opal nodules or “nobbies” from Lightning Ridge, NSW. (A–G) Potch opal showing a variety of sizes and white outer coatings and layers, Specimens GM-13A–GM-13G. (H) Precious opal nobby. (I) Translucent, amber-colored potch with a small dark inclusion of hollardite,  $\text{Ba}(\text{Mn}^{4+}_6\text{Mn}^{3+}_2)\text{O}_{16}$ , Specimen GM-13-I.

### 6.3. Septarian Networks, Reticulations, Melikaria, and Meniscus Structures

At Lightning Ridge, opal occurs in a seemingly endless variety of topologies. The shapes and textures apparently formed via a range of processes, none of which is well understood. Topologies include complex septarian patterns (Figure 5), in very fine and intricate honeycomb networks, in melikaria and rare counter-septarian structures, in shell-like laminae and husks, and in kernels and meniscus forms (“pools”, “cups”, and “dishes”), webs and “strings”, spots, spheroids, and botryoidal blobs.

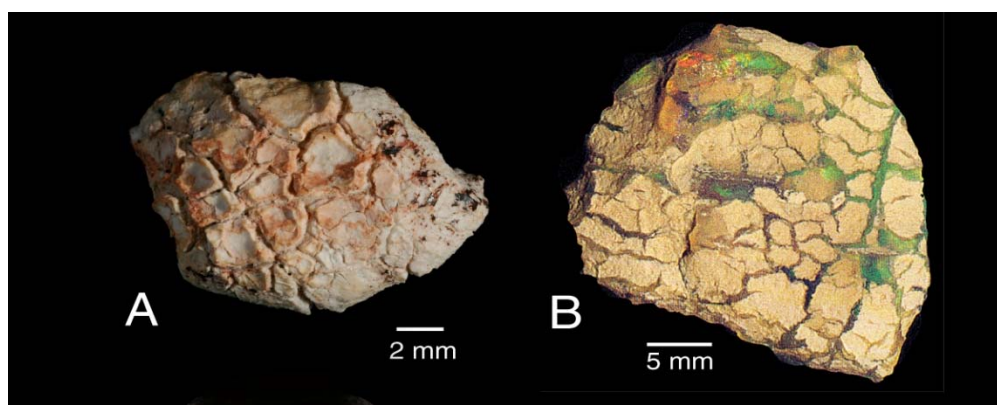


**Figure 5.** Septarian patterns in Lightning Ridge specimens. (A) Nodule of opaque potch (common opal) with unfilled surface fractures. Specimen LRF847. (B) Claystone with shrinkage fractures filled with dark potch and precious opal, photo (B) from [13].

Septarian patterns include intricate honeycomb networks, melikaria, and rare counter-septarian structures. The mechanism of septarian formation has been described in detail [47,48];

the term “melikaria” is used to describe features that have geometric patterns similar to septaria but lack a surrounding matrix [49].

Most of these structures represent delicate fractures that developed in silty clay as a result of dehydration. Very fine reticulations and “crinkled” textures commonly line cavities in plant fossils or in fissures between opalized structures and enclosing claystone. They are also seen sporadically on the outer surfaces of plant fragments, bivalve shells, and bones. These intricate boxworks have cavities that are empty as in melikaria. However, our observations suggest that some may have developed when gelatinous silica hardened and shrank away from cavity walls during desiccation, a result of the interaction between the tensile properties of silica gel and fine, hydroplastic claystone minerals. Other septaria may be infills of syneresis cracks formed by the dewatering of unconsolidated sediment.

As described later in this report, fine circular and polygonal patterns in certain water-worn nodules appear to represent the internal pneumatic composition of sauropod and theropod bone.

#### 6.4. “Ball-and-Pillow Structures” or “Foam Balls”

These rare and delicate topologies are highly enigmatic. They are small, extremely fragile, and do not survive the mechanized mining operation. “Ball-and-pillow” or soft-sediment deformation structures in clay sediments are known from many overseas locations. Herrmann and Maas [12] suggested that lace-like opal morphologies originated when opal filled porous intergranular spaces in permeable clastic sediment; the subsequent dissolution of the clasts is inferred to have left the opal as a relict material (Figure 6). Problematically, this explanation requires the sediment matrix to be unstable in composition relative to the opaline cement. An alternate possibility is that the openings were created by ebullition or bubbling during biogenic gas production at a time when the opal was gelatinous, and the surrounding claystone was very soft. Consistent with this scenario are certain widespread lithologies known locally as “biscuit band”, typified by numerous spherical and elliptical cavities that are commonly lined with potch. In this case, the most likely cause may have been sulfide gases, methane, or carbon dioxide released by the decomposition of organic material.

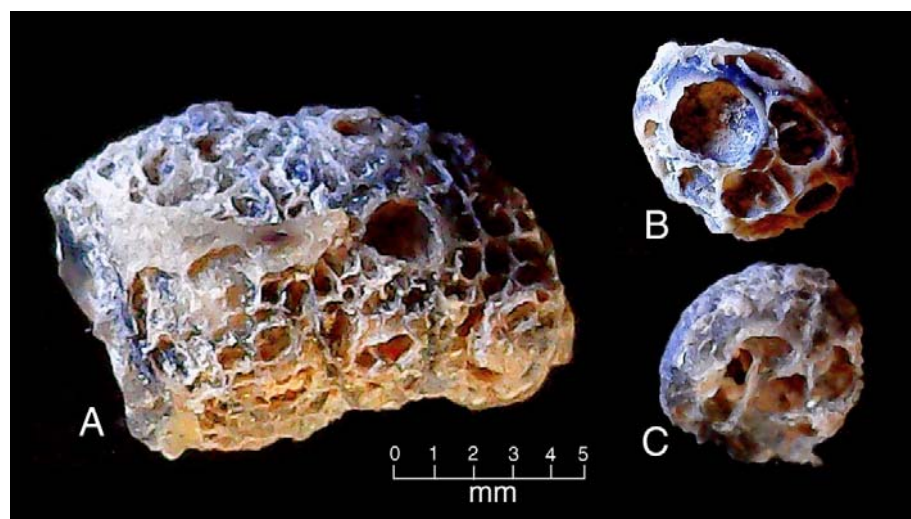


**Figure 6.** “Ball-and-pillow” structures or “foam balls”. These very fragile textures are enigmatic in origin. (A) Specimen GM-4B. (B) Specimen GM-4A. (C) Specimen GM-4C.

Topological progression is typical of the non-fossil structures described above. Forms that are intermediates or combinations of two or more of these types are abundant and multifarious. Importantly, however, this does not apply to invertebrate and vertebrate materials; shells and bones are commonly heavily corroded and weathered, but in general, they do not morph or degrade diagenetically into non-fossil structures.

### 6.5. Opalized Fossils

Lightning Ridge is an outstanding source of plant, ichnofossil, and invertebrate and vertebrate fossils preserved in opal. Many plant and invertebrate fossils are strongly compacted, but bones are usually perfect 3D casts (replicas), undistorted by compression or diagenesis, exhibiting variable degrees of pre-burial weathering. In translucent specimens, fine anatomical details, such as nutrient and nerve canals, may be visible inside the bone.

The fossilization process is a result of the clay-rich matrix, a malleable material that is favorable for molding the intricate shapes of organic remains. It is generally assumed that preservation as replacements or casts has eliminated internal details; however, a high percentage of bone specimens show clear microstructural features.

The locality yields a unique assemblage of freshwater and terrestrial remains, with rare marine elements. The fauna includes invertebrates (mollusks and freshwater crayfish) and an outstanding range of vertebrates such as fish, turtles, plesiosaurs, crocodiles, pterosaurs, dinosaurs, birds, and monotreme mammals.

Although the Cretaceous age of the opal-bearing sediment is evidenced by fossils, the timing of opal deposition and subsequent diagenetic changes evoke a complex paragenetic history. Our current research focuses on a diverse array of small specimens, with particular emphasis on plant remains, including wood, cones, and seeds.

## 7. Materials and Methods

The cataloging of samples used in our research are from the personal collections of coauthor ETS, numbered with the prefixes RM and GM. These will be accessioned into the public collection of the Australian Opal Centre at Lightning Ridge; those with the prefix LRF are already accessioned. Analytical work included optical microscopy, scanning electron microscopy, and X-ray diffraction, using facilities at Western Washington University, Bellingham, WA 98225, USA. Optical photomicrographs were taken using a 5-megapixel digital microscopic camera on a Zeiss Stereozoom binocular microscope (Zeiss Microscopy, White Plains, NY, USA) and with a USB-connected generic monocular zoom microscope with an internal 5-megapixel CMOS camera. SEM examinations were made using a Tescan Vega-3 electron microscope (Tescan, Brno, Czech Republic) equipped with an Oxford energy-dispersive X-ray detector running AzTek software (Oxford Instruments, Abingdon, UK). Specimens were attached to a 1 cm diameter aluminum stub, sputter-coated with Pd to provide electrical conductivity.

## 8. Paleontology

Opal mining at Lightning Ridge began in the late 1880's; since then, fossils have been recovered as a by-product of mining. In the early years, fossil finds attracted scant attention, and the high value of precious opal resulted in the destruction of many fossils that were cut into gemstones (Figure 7), a practice that continues even today. By 1912, lungfish tooth plates, osteoderms, and a crocodile jaw fragment were lodged with the Australian Museum in Sydney. However, the earliest on-field report is of vertebrate fossils recovered from a shaft sunk in 1909 that were sent to the British Museum. Although reported in 1910 as the remains of a megalosaurian dinosaur [50], they were unstudied until 1932, when German dinosaur specialist Freidrich von Heune described four bones as representing three new species of theropod dinosaur: *Walgettiosuchus*, *Rapator*, and *Fulgurotherium* [51]. Subsequently, dinosaur genera identified from Lightning Ridge include ornithopods such as *Weewarrasaurus* [52] and *Fostoria* [9], along with megaraptorotids [53] and noasaurids [54], theropods, and sauropods [55].

Lightning Ridge fossils became famous in the early 1980s with the discovery of the monotreme mammals *Steropodon* [56] and *Kollikodon* [57]. The fossil fauna was reported and illustrated by Smith [13] and more recently has been the subject of intensive research, primarily by collaboration between the Australian Opal Centre at Lightning Ridge and the Department of Earth Sciences at the University of New England, Armidale, NSW.

The locality yields a unique assemblage of freshwater and terrestrial forms, with rare marine elements. At a paleolatitude of ~60° S [10] with low winter light, temperate conditions are inferred by the presence of warm-climate forms (viviparid snails, crocodylians, and sauropods).

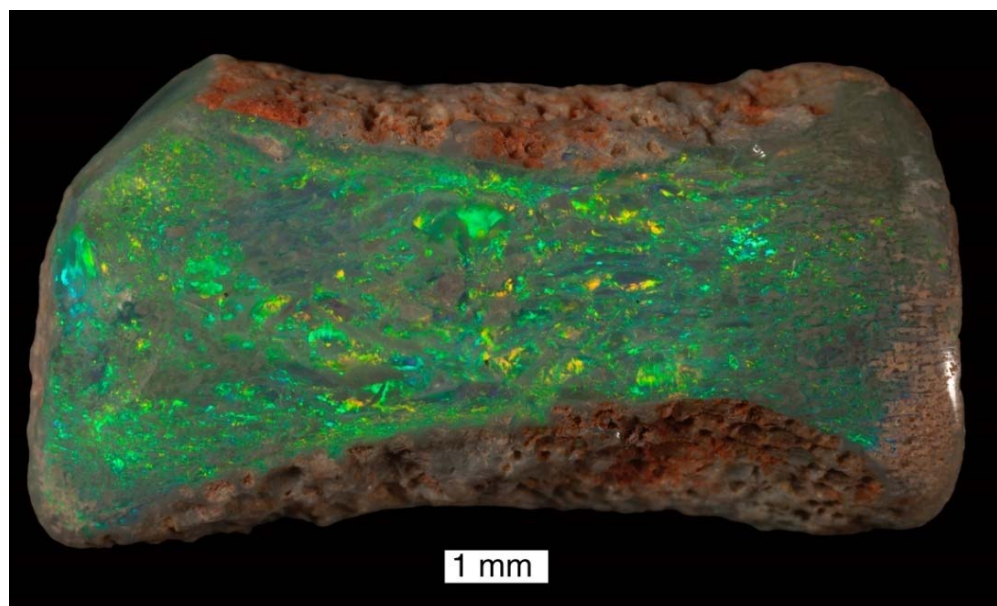


**Figure 7.** LRF3589. Dinosaur vertebra mineralized with precious opal. Note that the trabecular bone microstructure is preserved throughout the specimen. The lower surface has been polished to reveal the opal color, which has destroyed some of the scientific value. Photo by Robert A. Smith.

## 9. Results

Our paleontology research is based on the study of the remains of invertebrates, vertebrates, and plants. Most specimens are small, and microscopic analysis is an important element of our studies.

### 9.1. Evidence from Plant Fossils

The most abundant fossils at Lightning Ridge are opalized plant remains, which include wood (small logs, branches, twigs), “pine cones” (strobili and sporophylls), cone scales and cone cores, and seeds. Many are corroded, weathered, compacted, and distorted, with no anatomical details; others are crisply preserved and immediately identifiable, characterized by remnants of wide leaf bases that form irregular diagonal surface ridges and paleoinclusions that are squarish or rectangular. Although they are a major component of the paleochannel debris, these materials have previously received little study, and taxonomic affinities, even of the major groups, are unresolved. They have provided important clues for understanding the mineralization sequence.

In general, the fossilization of plant tissues follows multiple pathways, with major differences between the preservation of leaf remains and stem or trunk tissues. Foliage is typically preserved as compressions or impressions in fine sediments. Commonly, the tissue has been degraded to produce a dark film, but it is not uncommon for the leaf cuticle to be preserved in its original form. In other cases, the leaf shape is preserved as an imprint, with no relict organic matter. The fossilization of leaves generally occurs rather rapidly, a necessary condition for thin tissues that are susceptible to degradation.

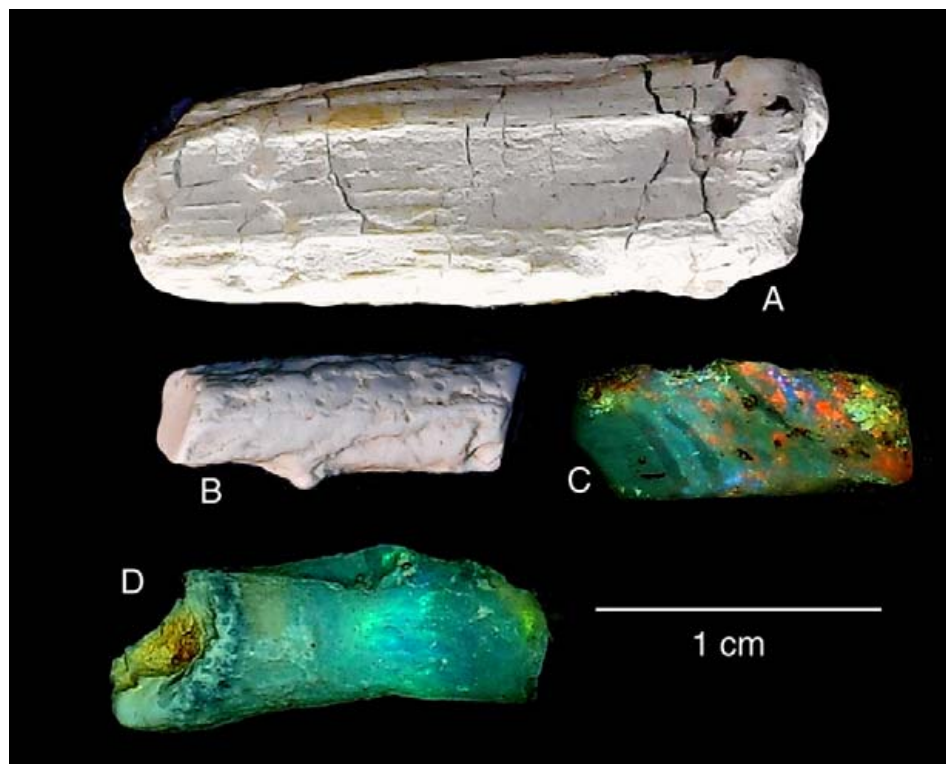
The preservation of ancient wood may be very different. The fundamental purposes of wood are to provide fluid transport and strength and rigidity that allow a tree trunk to support a leaf crown at a height that favors exposure to sunlight. These factors are important during fossilization. Buried wood tends to retain a three-dimensional shape, and natural permeability allows the entry of mineral-bearing groundwater that may result

in petrifaction. These characteristics hold true regardless of the specimen size, being applicable for large logs, wood fragments, and small twigs.

A major variable is the time required for petrifaction, a situation where there is no uniform rule. Wood immersed in a hot spring may become mineralized quickly because of the high concentration of dissolved silica. More commonly, wood is mineralized in a series of stages spanning a long time interval.

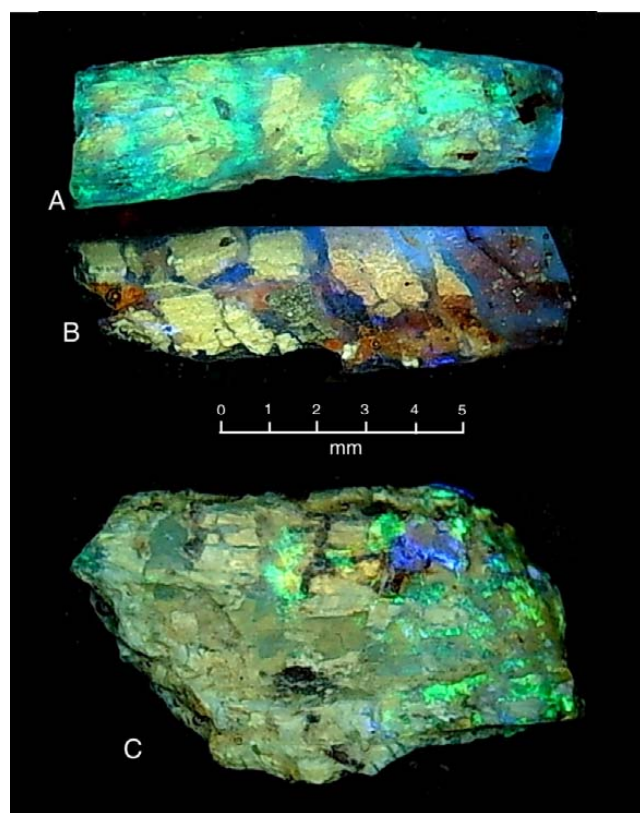
If wood is buried in impermeable sediment that prevents the entry of mineral-bearing groundwater, mineralization may not occur. This phenomenon is generally found when wood is buried in clay-rich sediment. Examples include the Eocene and Oligocene mummified woods that occur abundantly on the islands of the Canadian Arctic and in various locations in Europe and North America [58,59].

Fossil wood is commonly described as being “permineralized”, where original tissue is entombed within silica or other minerals. More commonly, petrifaction is the result of replacement, where only small amounts of relict organic matter are preserved [60]. We observed no permineralized wood at Lightning Ridge. Plant fossils are primarily opal casts of small twigs or wood fragments, though large specimens have been found. These wood casts may consist of potch, precious opal, or a combination of the two (Figure 8).

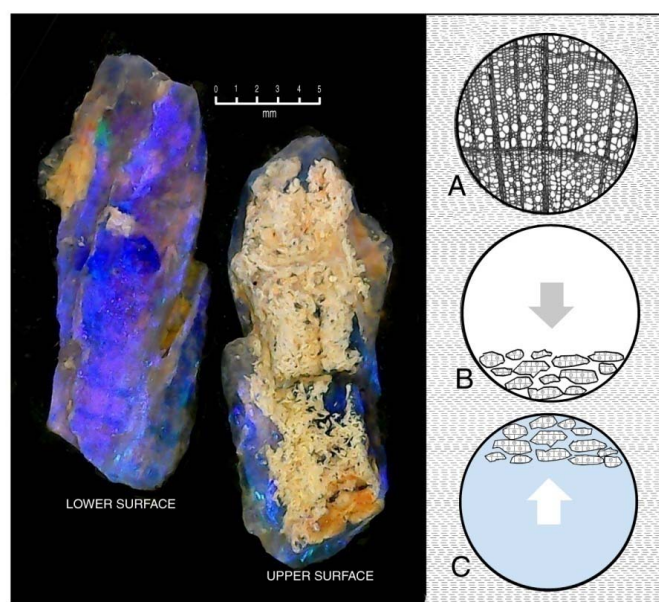


**Figure 8.** Opal wood cast from Lightning Ridge, NSW. (A) Wood fragment, Specimen RM-36, and (B) small twig, Specimen RM-37. Both are composed of potch opal. (C,D) Small twig casts composed of precious opal, Specimens RM-30, RM-31.

Very commonly, wood casts that are composed of translucent opal contain fragmental inclusions (Figure 9). These often show a geopetal distribution, indicating that the original wood was buried in a horizontal position; gravity caused the included fragments to settle to the bottom of the mold that was left when the original organic matter was destroyed, but the buoyancy of these particles caused them to float to the top of the chamber in the presence of silica-bearing fluids. The result was the silicification of the degraded wood in a chamber that was otherwise opal-filled (Figure 10).

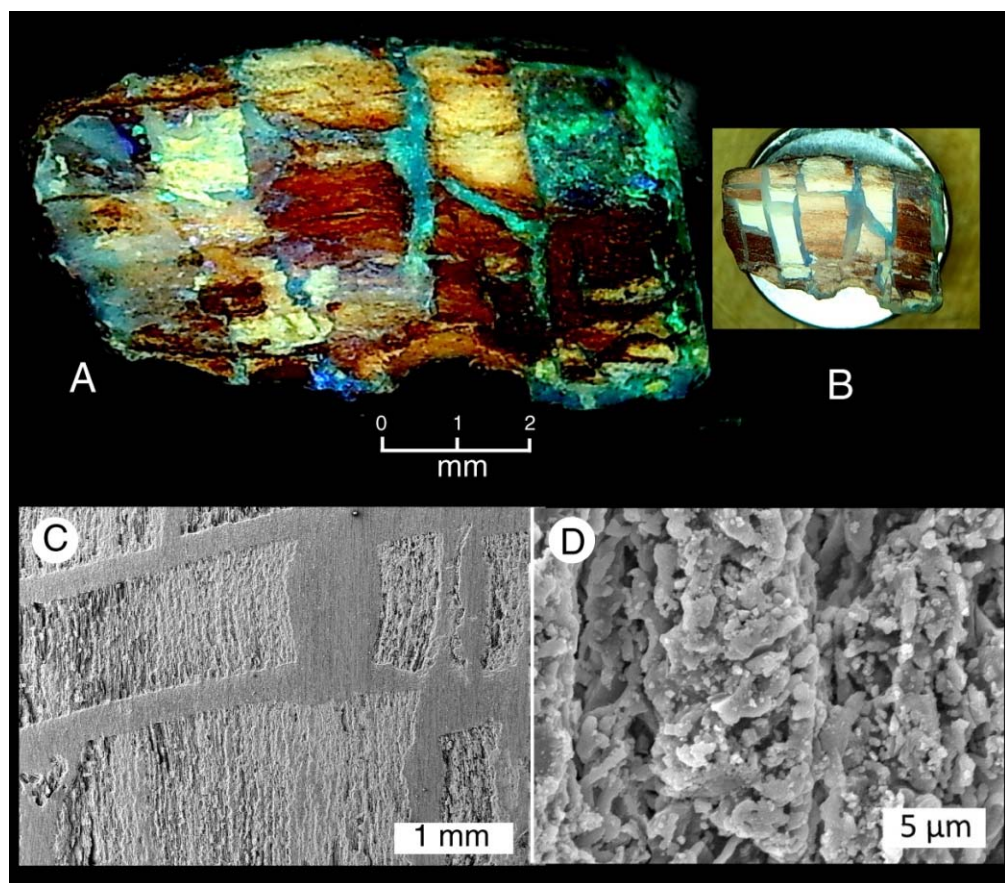


**Figure 9.** Small wood fragments preserved as precious opal casts containing abundant angular inclusions. (A) Specimen RM-30B. (B) Specimen RM-30A. (C) Specimen RM-30C.



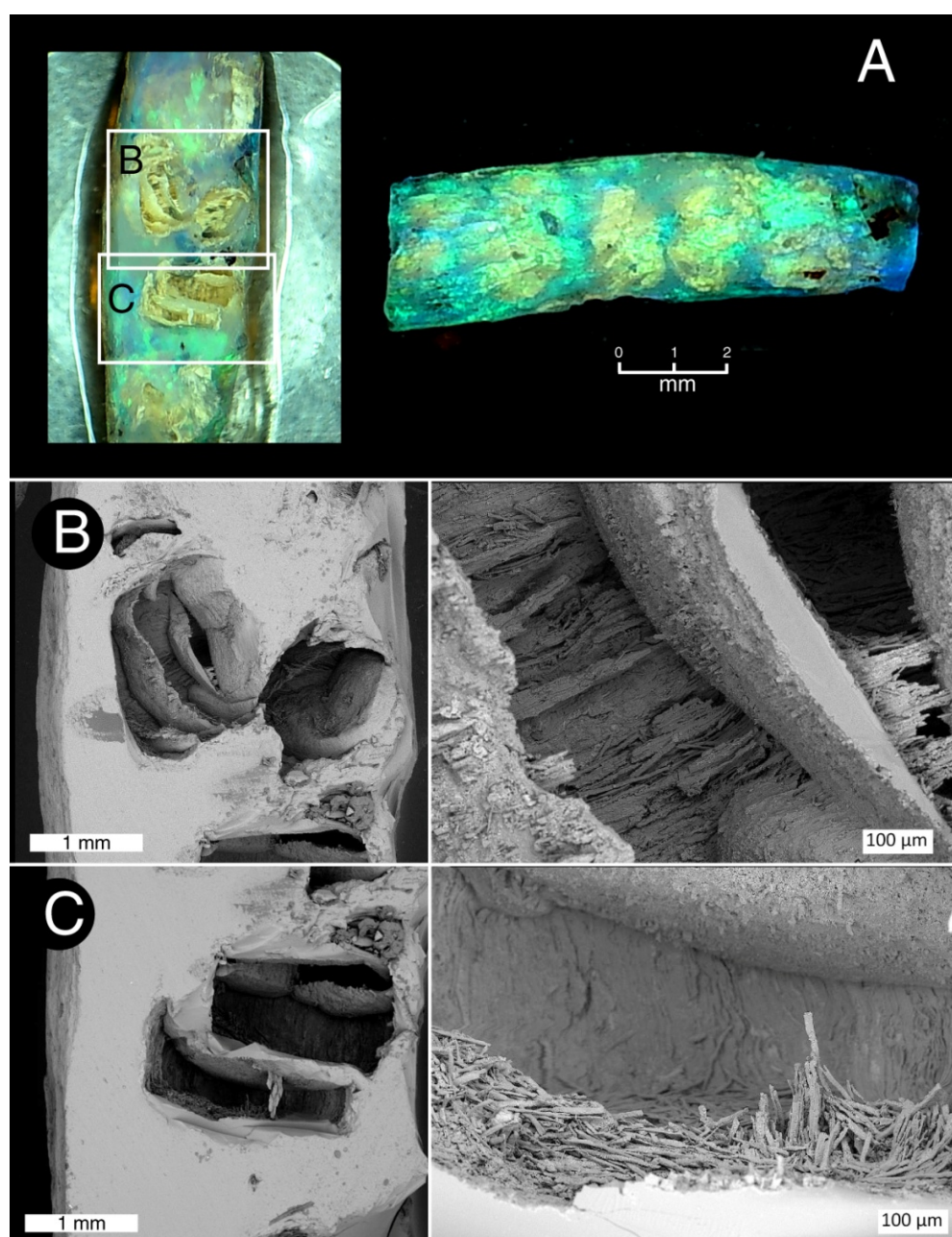
**Figure 10.** Small wood fragment mineralized with precious opal. Internal inclusions show geopetal textures, indicating paleohorizontal. These pieces are commonly found silicified in place on the sole of the steel band, with the inclusions at the top of the opalized cavity. (A) Fossilization begins when a wood fragment is buried in clay-rich sediment. (B) Degradation produces fragments that settle to the bottom of the empty chamber by gravity. (C) Filling of the chamber with silica-rich groundwater causes the wood fragments to float, where they become opalized at least in their marginal zones. Specimen GM-8.

The light color of the angular inclusions was initially presumed to represent fragments of claystone that were transported into the cavity as it was being filled with gelatinous opal. Microscopic examination disproved this hypothesis; in these opal wood casts, the inclusions typically represent mineralized tissue. Figure 11 shows a specimen that contains abundant fragments of wood that has been replaced by potch. This texture appears to represent a wood fragment that was initially mineralized and subsequently fractured or shattered to produce intervening spaces that later became filled with precious opal. This composition is indicative of two episodes of opal precipitation.



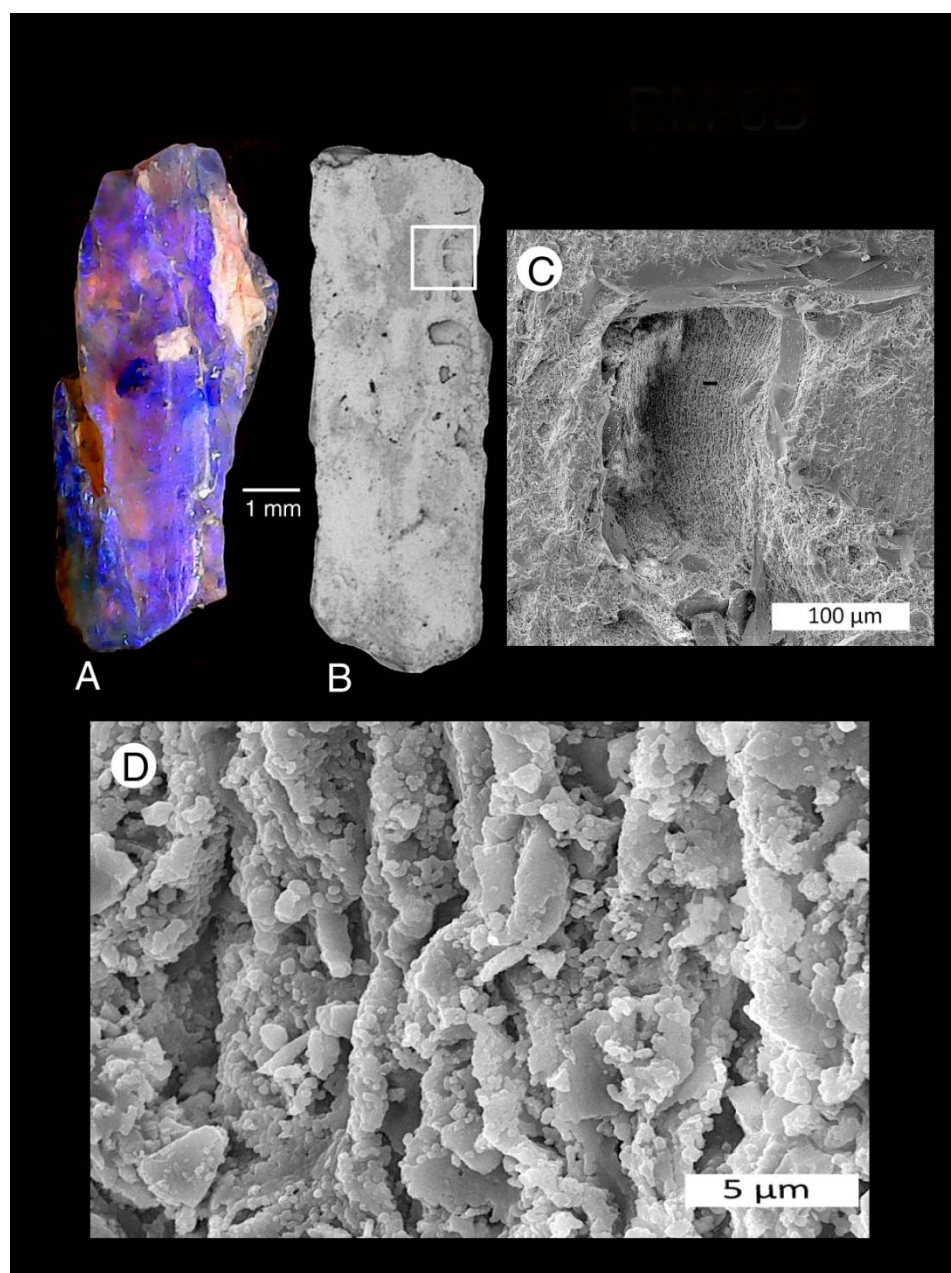
**Figure 11.** Wood specimen where external form is a cast, but the overall composition consists of brecciated blocks of potch-opalized wood, separated by precious-opal zones. (A) Transmitted light optical photomicrograph. Specimen RM-30C. (B) Specimen glued to a 1 cm diameter aluminum stub for SEM, with the upper surface ground flat and polished to reveal the internal structure. (C) Low-magnification SEM image reveals geometric blocks of opalized wood with intervening spaces filled with amorphous opal. (D) High-magnification view of three adjacent wood cells that were replaced by Opal-AG potch.

Figure 12 shows a different process of fossilization. In this specimen, polished, flat surfaces show that the angular inclusions have the form of hollow “boxes” that were created when wood fragments had only incipient mineralization at the time when the mold became filled with opal. These inclusions contain scant quantities of silicified cells, which in some instances have collapsed to the floor of the cavity (Figure 12B). The walls of the “box” show a thin zone of vitreous opal.



**Figure 12.** Cast of a small twig composed of precious opal, containing opaque inclusions. Specimen RM-30B. (A) Image shows the original specimen on the right. Left image shows the polished, flat surface showing SEM image areas (B,C). (B) Inclusion is in the form of a hollow area with thin opal septa within a cavity that contains sparsely preserved, silicified wood cells. (C) A cavity pair has thin outer walls of dense amorphous opal that contain individual, silicified wood cells that show gravitational collapse.

Figure 13 shows another opal wood cast that has the “hollow box” morphology. In this specimen, the preservation of relict wood is limited to thin “wallpaper” zones on the inner walls of each cavity. Seen in longitudinal orientation, the silicified cells have distorted shapes that suggest the original wood fragments were degraded at the time that opal was deposited within the mold cavity. The box-like spaces are surrounded by a thin zone of vitreous opal. This is a common feature of opalized wood specimens and presumably is the cause of the opaque, white appearance of the inclusions when specimens are viewed by the naked eye.



**Figure 13.** A twig fragment mineralized with translucent precious opal. Light-colored angular inclusions have an “empty box” structure, with wood cell textures preserved on the cavity walls. (A) Transmitted light optical microscope image. (B) Back-scattered electron (BSE) SEM image. The area of (C) is shown as a white rectangle. (C) The voids have a thin, vitreous wall that preserved the wood cell structure. (D) High-magnification SEM image reveals that wood cells have been replaced by opal. The distorted shapes of these elongated cells suggest that the wood was in a state of decomposition at the time of silicification. Specimen RM-8B.

The Lightning Ridge sandstones and claystones also contain numerous examples of a peculiar form of preservation in which individual wood cells or tracheids have been replaced by colorless translucent opal, with intercellular spaces remaining unmineralized. Lying in parallel rows, the tracheid endocasts form small bundles with a fibrous texture (Figure 14). Like the “foam balls” discussed previously, they are extremely fragile and do not survive mining machinery. The tracheids are held in longitudinal compartments inside plant stems and are presumed to represent small regions inside decomposing wood where local geochemical conditions induced highly mobile silica to flood the vascular tissues and

harden before the decay of the cell walls. In some instances, the wood cells experienced degradation prior to mineralization. In other cases, the cells were in pristine condition at the time of their replacement with Opal-AG.

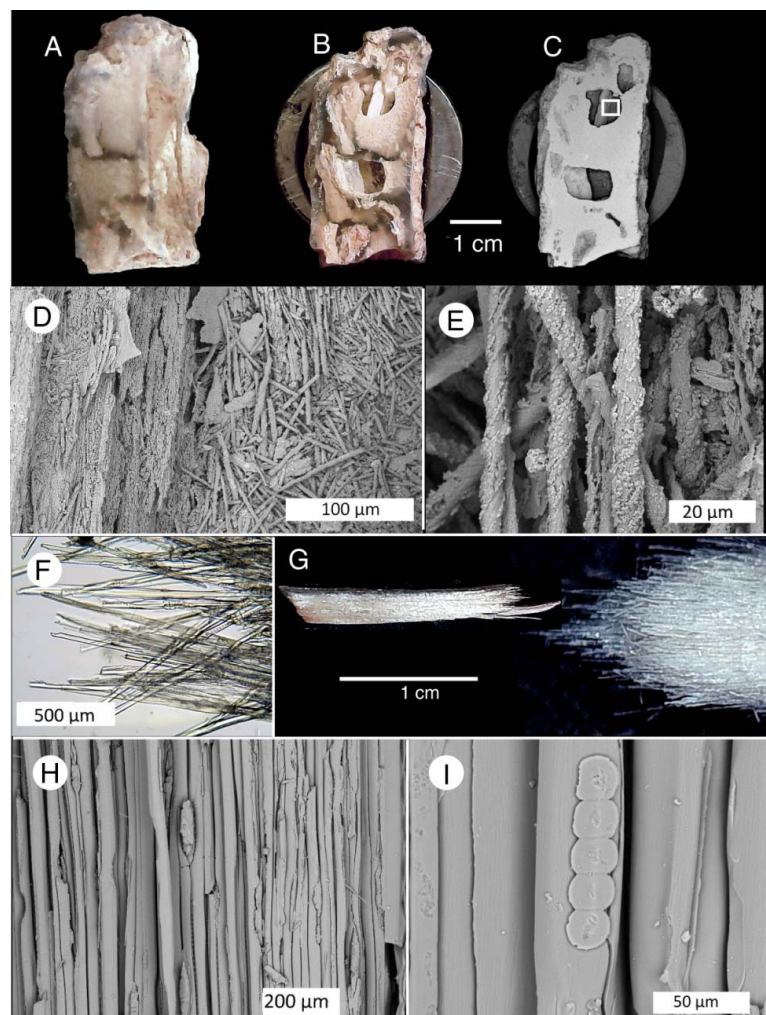


**Figure 14.** Opalized wood from Lightning Ridge showing the preservation of individual cells. (A) Fossil wood specimen GM-6C prior to preparation. (B) Specimen mounted on an aluminum stub and ground and polished to reveal internal inclusions. (C) SEM BSE image showing inclusions as partially empty cavities. The white rectangle shows the area illustrated in (D), where silicified cells have both an ordered (left) and disordered (right) structure. (E) These cells underwent degradation prior to replacement by silica. The spiral morphology is indicative of wood that has experienced fungal deterioration. In some specimens, tracheids were silicified while they were still in a pristine condition. (F) Transmitted light photomicrograph of an opalized cell lumen cast, Specimen RM-43. (G) Reflected light view of a bundle of parallel cells and a transmitted light, Specimen RM-42. (H) SEM BSE image of Specimen RM-42 showing silicified cells with unmineralized intercellular spaces. (I) Higher-magnification SEM image documents the preservation of casts of intervessel pit chambers, with bordered margins that are characteristic of gymnosperm wood.

Other plant fossils include small “pine cones” or strobili from gymnosperms (Figure 15). These preserve a delicate external morphology, but those that were collected from machine-washed sediment have eroded shapes (Figure 15A–C). Specimens collected directly from the original host matrix preserve the delicate scale structure (Figure 15D,E), evidence of the ability of clay-rich sediment to produce molds that capture exquisitely fine details.

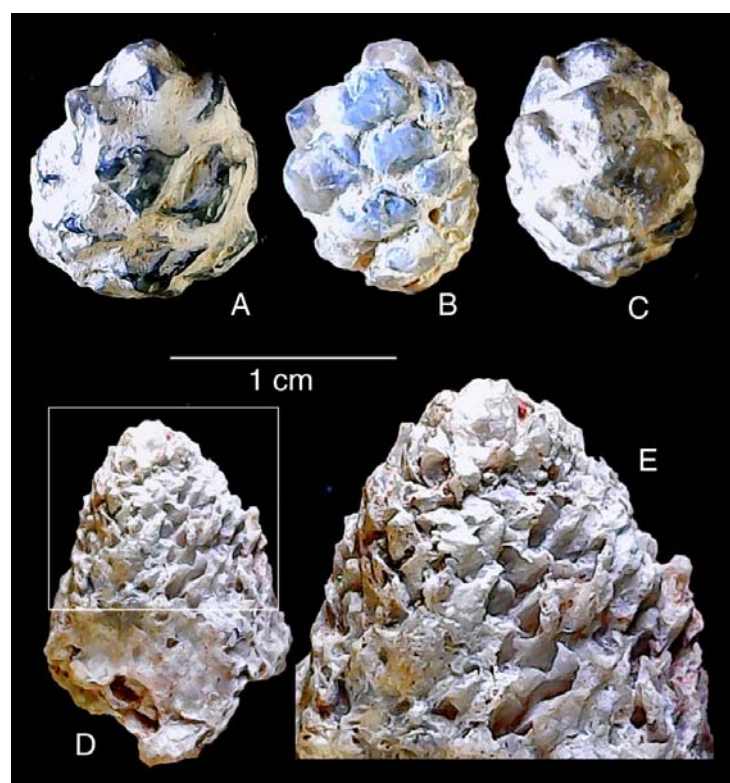


**Figure 15.** Opal-AG casts of conifer cones. (A–C) Specimens that have undergone mechanical washing or processing that has rounded and abraded the cone scales, removing fine surface features. Specimens GM-31A-C. (D) View of a specimen that was not machine processed. Individual cone scales are sharp and extend to the central cone core, but they are opal casts not permineralized tissue. (E) Enlargement of area outlined in the previous photo. Specimen RM-31.

Opalized seeds are another type of plant tissue from the Finch Claystone (Figure 16). The central areas of these specimens are commonly clouded with inclusions; further microscopy work is needed to determine if any internal reproductive features are preserved. Evidence of non-flowering plants includes a detailed cast of a fern rhizome (Figure 17).



**Figure 16.** LRF833. Early Cretaceous–Cenomanian seeds from Lightning Ridge preserved as opal casts. Photograph by Robert A. Smith.

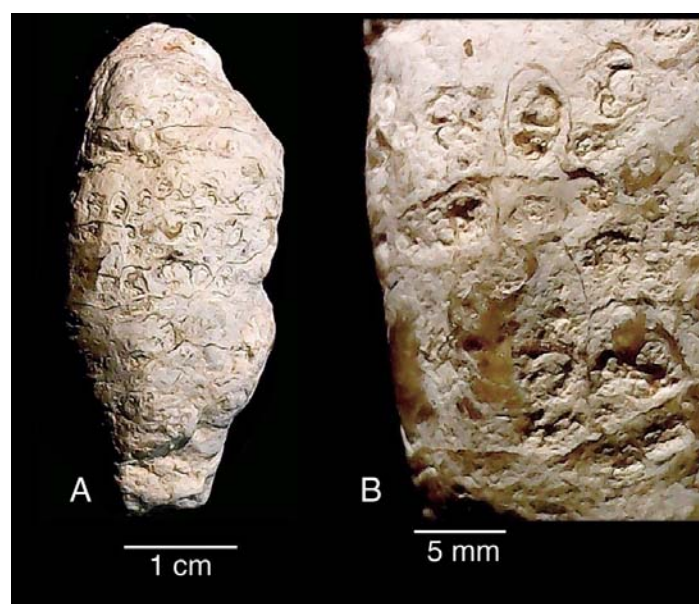


**Figure 17.** Opal cast of a presumed fern rhizome. The specimen is delicately reticulated with fine subcircular lines representing rows of curled frond bases that extend inward to the cylindrical central core. (A) Overall view. (B) Close-up view showing the preservation of surface details. Specimen RM-35.

Among the most puzzling Lightning Ridge fossils are specimens that have reticulate patterns of thin septa that surround empty areas that commonly contain even finer networks of “secondary” septa and cavities. It is difficult to interpret these topologies; however, given that some are fully enclosed inside flattened plant stems, such specimens are interpreted here as representing the opalization of the soft pith-like medullary tissue of vascular plants (i.e., angiosperms) (Figure 18).

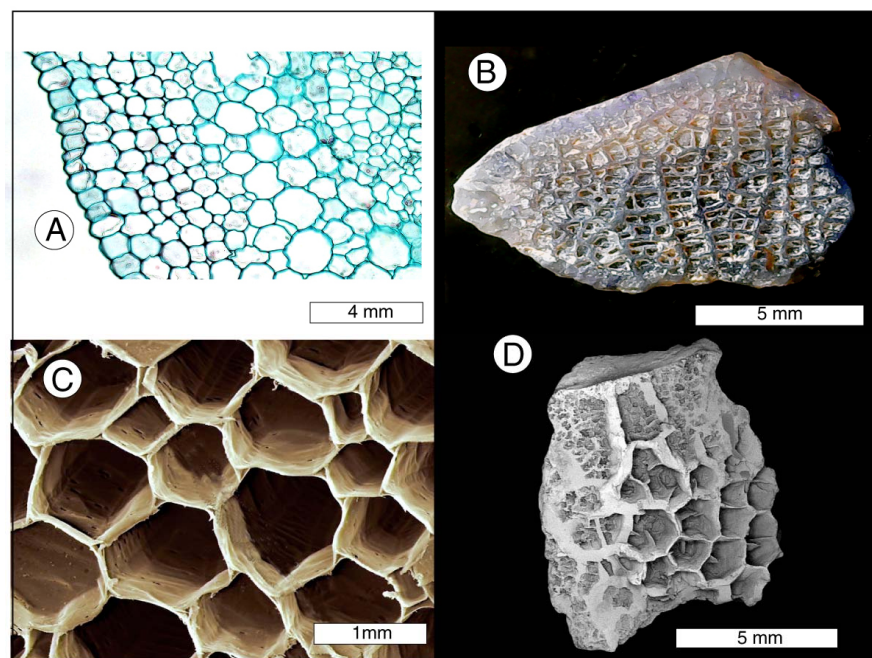


**Figure 18.** Reticulate opal patterns in small Lightning Ridge specimens may represent stem tissue in herbaceous angiosperms. (A) Modern *Richinus*. Image from [61], used with open access permission. (B) Lightning Ridge Specimen GM-9C. (C) Modern *Cannabis* (SEM image). (D) Lightning Ridge Specimen GM-25.

### 9.2. Evidence from Invertebrate Fossils

By far the most common fossils are small plant fragments, but freshwater invertebrates are locally abundant by number, volume, and weight, comprising a diverse array of pelecypods (predominantly mussel shells), small gastropods (Figure 19), and crayfish remnants.

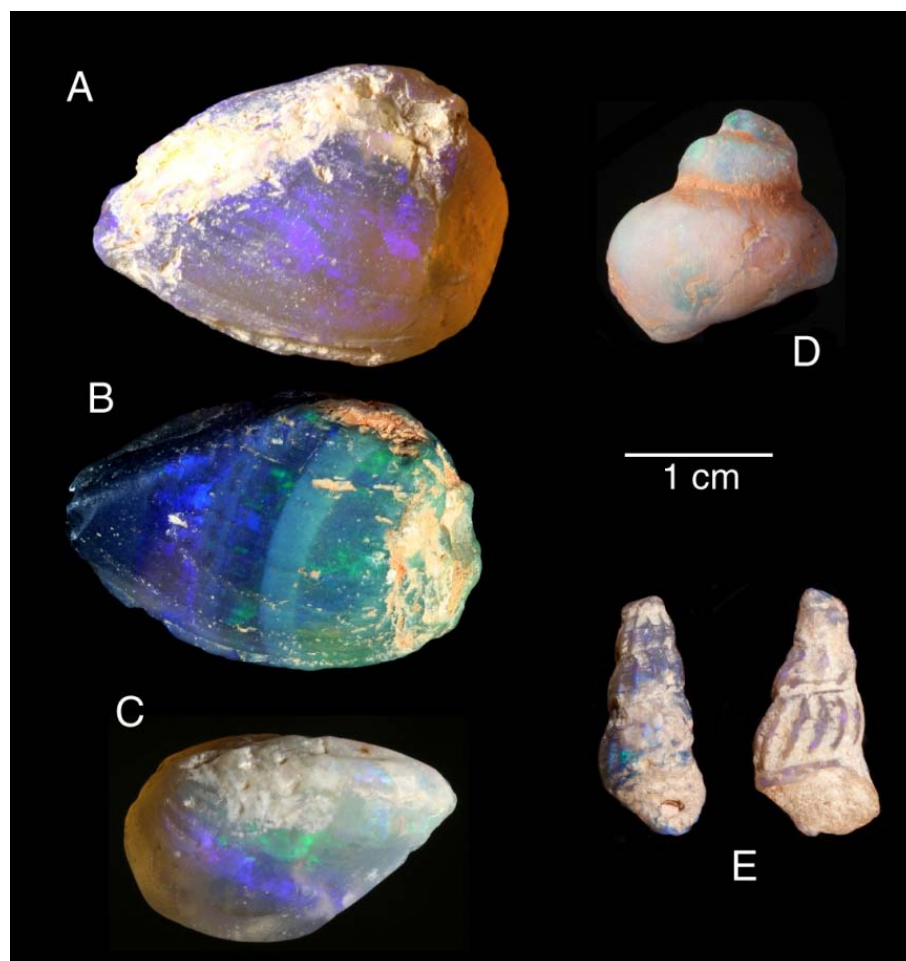


**Figure 19.** Opalized freshwater mollusks from Lightning Ridge, NSW. (A) LRF557. Cast of unionid mussel shell mineralized with translucent blue-purple opal. (B) LRF618. Mussel shell mineralized with layers of opaque black potch between “bars” of translucent precious opal. (C) LRF1054. Mussel shell in translucent blue, green, and mauve opal. (D) LRF1413. Viviparid gastropod snail; shell preserved in turquoise opal; internal cavity filled with white claystone (E) LRF1828. Thiarid gastropods *Melanoides* sp. composed of precious opal with claystone inclusions. Photographs by Robert A. Smith.

Opalized crayfish gastroliths are referred to locally as “yabby buttons” (Figure 20). In freshwater crayfish, these disc-shaped objects form as deposits of calcium carbonate in the anterior region of the carapace, providing a mineral reservoir for hardening the new exoskeleton after molting [13,62]. On a worldwide basis, they are rare in the fossil record, and these opalized specimens are found only at Lightning Ridge.

In summary, calcareous invertebrate fossils in the Finch Claystone have been preserved as opal casts. They lack internal anatomical detail and preserve only the external shape. The fossilization of these objects requires the dissolution of calcium carbonate, with diagenetic conditions of acidic pH (Figure 21). The rate of carbonate dissolution is time indeterminate; at low pH, calcite dissolves rapidly, but at higher pH, carbonate material can persist for tens of millions of years, as evidenced by the multitude of ancient

mollusk shells at worldwide localities that retain a pearly luster. The filling of the empty molds left by the dissolution of calcium carbonate would have required the availability of groundwater carrying dissolved silica and permeability of the host sediment to allow solutions to reach the empty spaces.

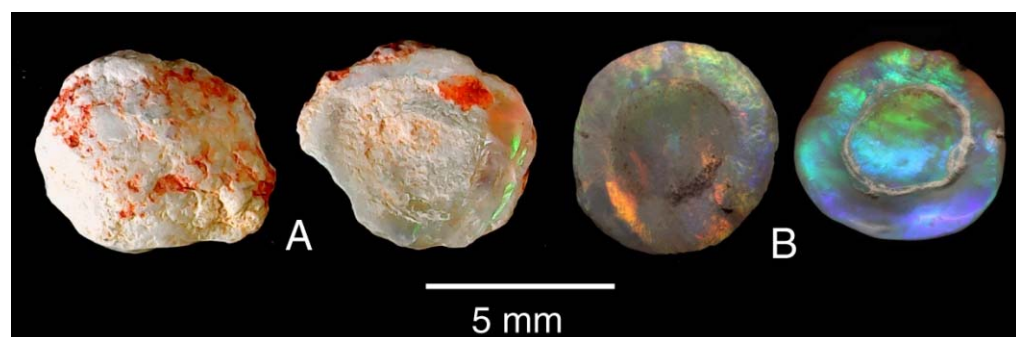


**Figure 20.** Crayfish gastrolith casts or “yabby buttons”, a Lightning Ridge specialty. (A) GM13. Specimen in amber and white potch, Specimen LRF 3589, (B) and in precious opal, Specimen LRF0435. Photographs by Robert A. Smith.

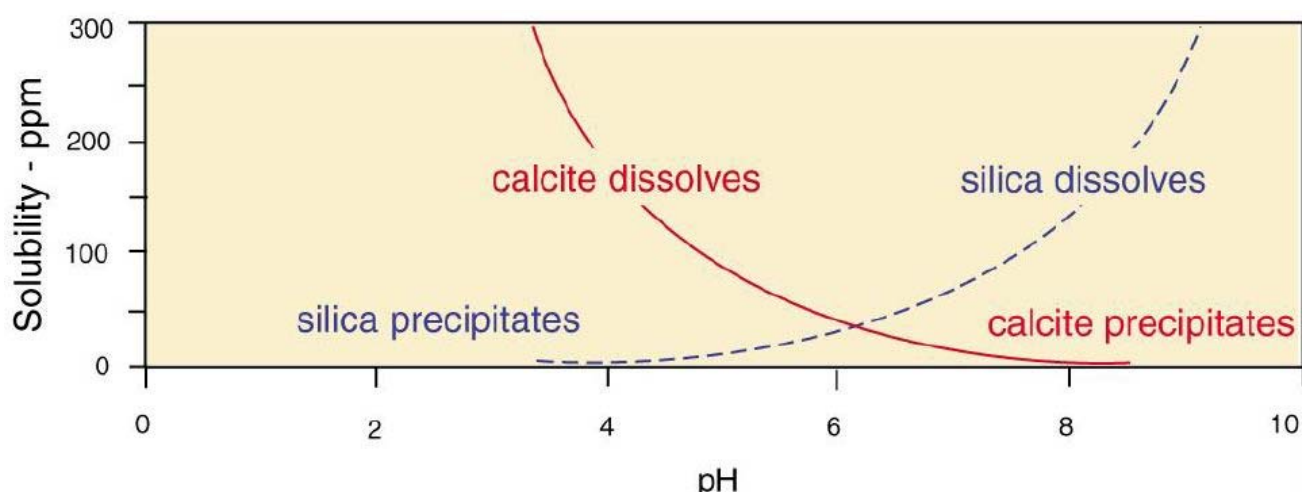


**Figure 21.** Stability range for silica and calcite under near-surface conditions. Data adapted from [63,64].

### 9.3. Evidence from Vertebrate Fossils

Vertebrate bone fossils at Lightning Ridge commonly consist of casts of teeth or bones, where the original organic material was degraded, leaving an empty cavity that was later filled with opal or potch (Figure 22). However, many examples show some degree of preserved cellular anatomy (Figure 22E–H). In both instances, the fossils consist only of opal, with no detectable relict organic matter.

The amount of time needed for the loss of the original collagen and bioapatite is indeterminate, but it was probably a rather slow process. Fully opalized plesiosaur bone has been described from the opal beds of the Bulldog Shale at Coober Pedy, but ichthyosaur bone from the Moon Plain near Coober Pedy from the same formation contains bioapatite that has been partially replaced by magnesium calcite. Plesiosaur bones from Andamooka (Wallumbilla Formation) contain Opal-AG and quartz but no apatite [65,66]. These occurrences are evidence that rates of bone dissolution are locally variable.

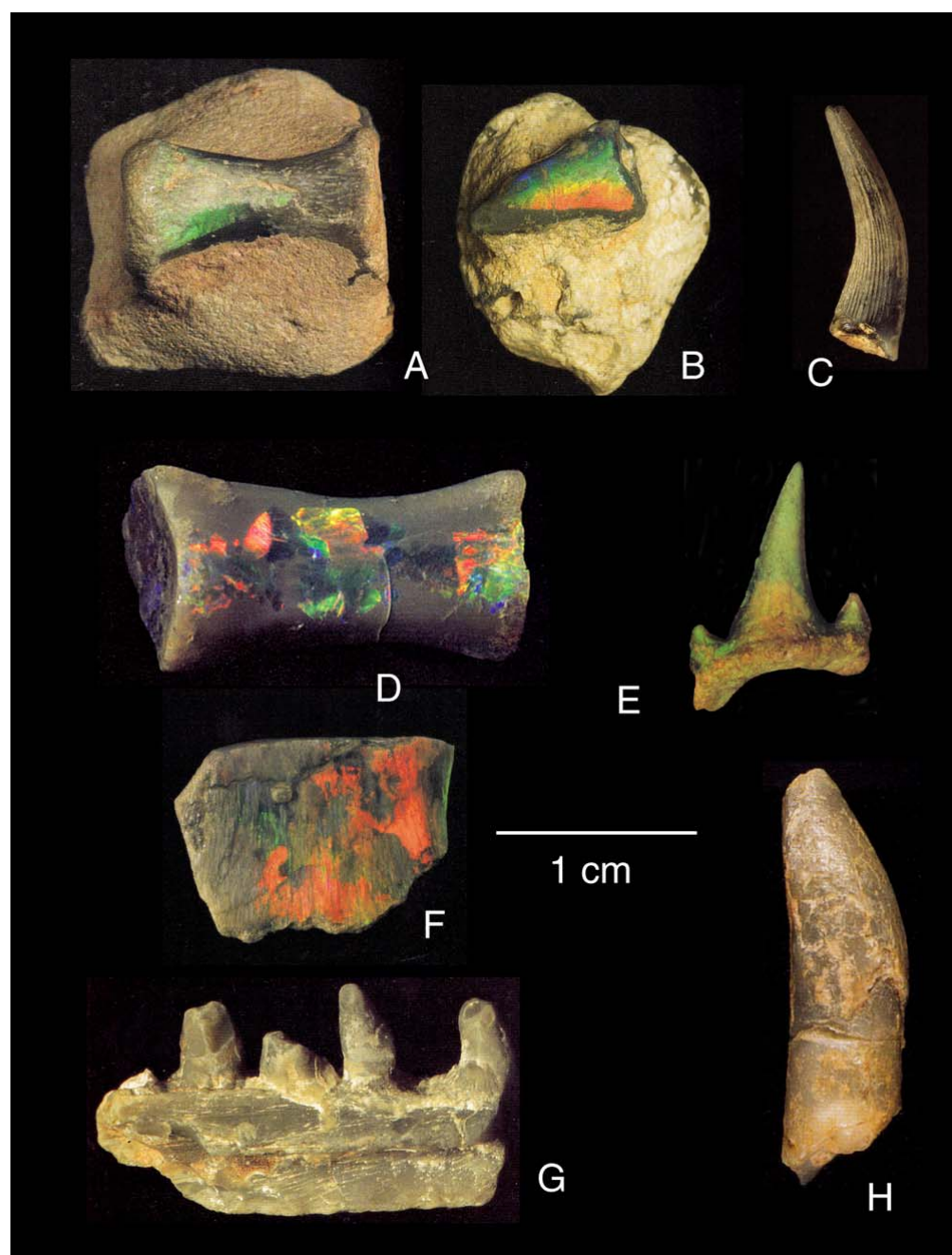


**Figure 22.** Vertebrate fossils from Lightning Ridge. (A) Crocodile vertebra. (B) LRF3064. Crocodile tooth. (C) Elasmosaurid tooth. (D) Dinosaur caudal vertebra. Cody Opals P/L Melbourne. (E) LRF4334. Shark tooth. (F) LRF618. Turtle shell fragment. (G) Fish jaw with teeth. (H) Sauropod tooth. Australian Museum Specimen AMF66770. Photographs by Robert A. Smith [13]. (A,C,G) are privately owned.

Non-opalized fossils have not been found in the Griman Creek Formation at Lightning Ridge. However, Dr Phil Bell provided two samples of ichthyosaur bone from the GCF at Bymont Station, Surat, Queensland, ~160 km NE of Lightning Ridge. SEM/EDS analyses reveal that the Surat bone consists of bioapatite, with no trace of mineralization. Microscopic images show that the original cellular anatomy is well-preserved (Figure 23). This is evidence that under the right conditions, bone buried in fine-grained sedimentary rock can remain intact for 100 million years.

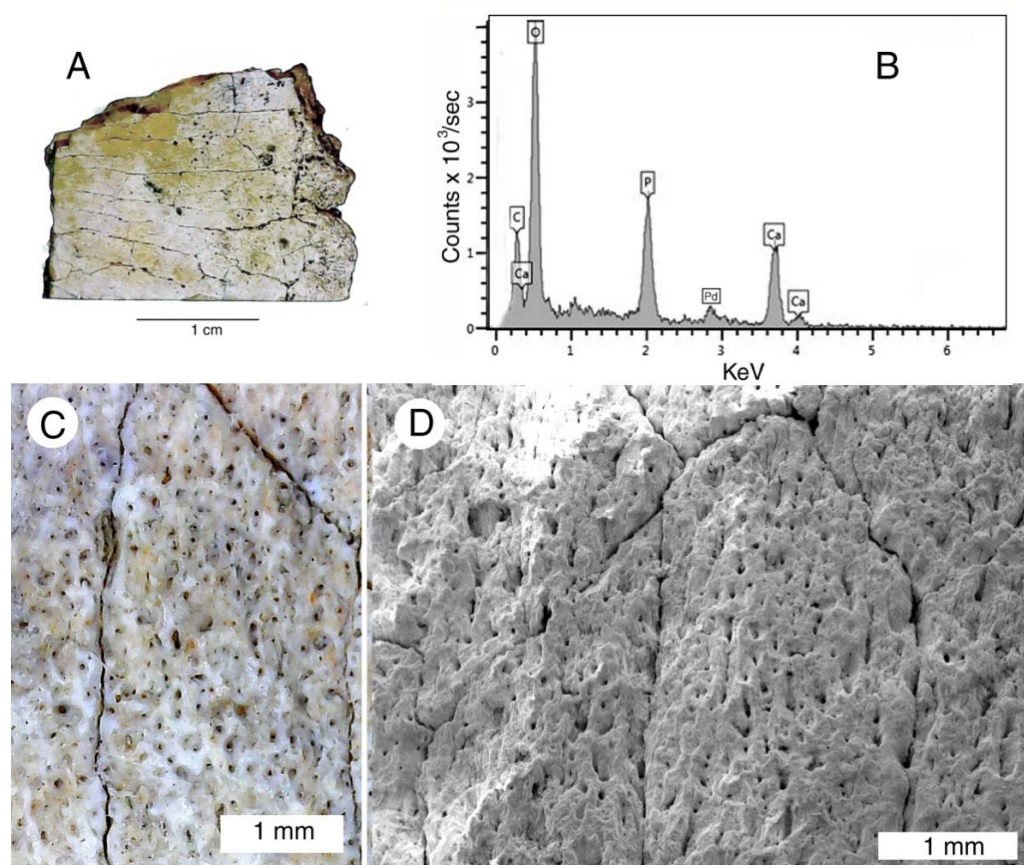


**Figure 23.** Ichthyosaur bone from the Early Cretaceous–Cenomanian Griman Creek Formation showing original bioapatite composition. (A) Bone fragment from Bymont Station, Surat, Queensland. (B) SEM/EDS spectrum showing calcium phosphate composition, with a small amount of carbon from organic matter. The PD peak is from the coating applied to provide electrical conductance. (C) Optical microscope image showing well-preserved osteology. (D) SEM image showing similar anatomical features as in (C).

Pneumatic theropod vertebrae are known from Lightning Ridge [67], and certain enigmatic Lightning Ridge specimens with fine, reticulated silica patterns are here interpreted as fragments of bone. Pleurocoels or camellate textures develop inside the vertebrae and limb elements of large dinosaurs and are also characteristic of birds and pterosaurs and reported for non-avian theropods and sauropods [68–71].

It is not always easy to distinguish between silicified plant-stem tissue and bone specimens that exhibit internal pleurocoel or spongiform composition. However, as a general rule, cell walls in opalized bone are thicker, with clay-rich sediment filling the pneumatic spaces (Figure 24). This morphology indicates a complex mineralization process. The first step involved the degradation of the bioapatite/collagen structure, leaving molds that allowed opal to replicate the cellular architecture. Fine-grained sediment then enclosed the bone and filled the void spaces. The subsequent dehydration of this clay-rich material produced complex shrinkage cracks around the pleurocoels that became filled with opal during a later episode of silica deposition. Elemental mapping by SEM/EDS clearly shows the distributions of Si and Al between the various mineral phases (Figure 24C,D).

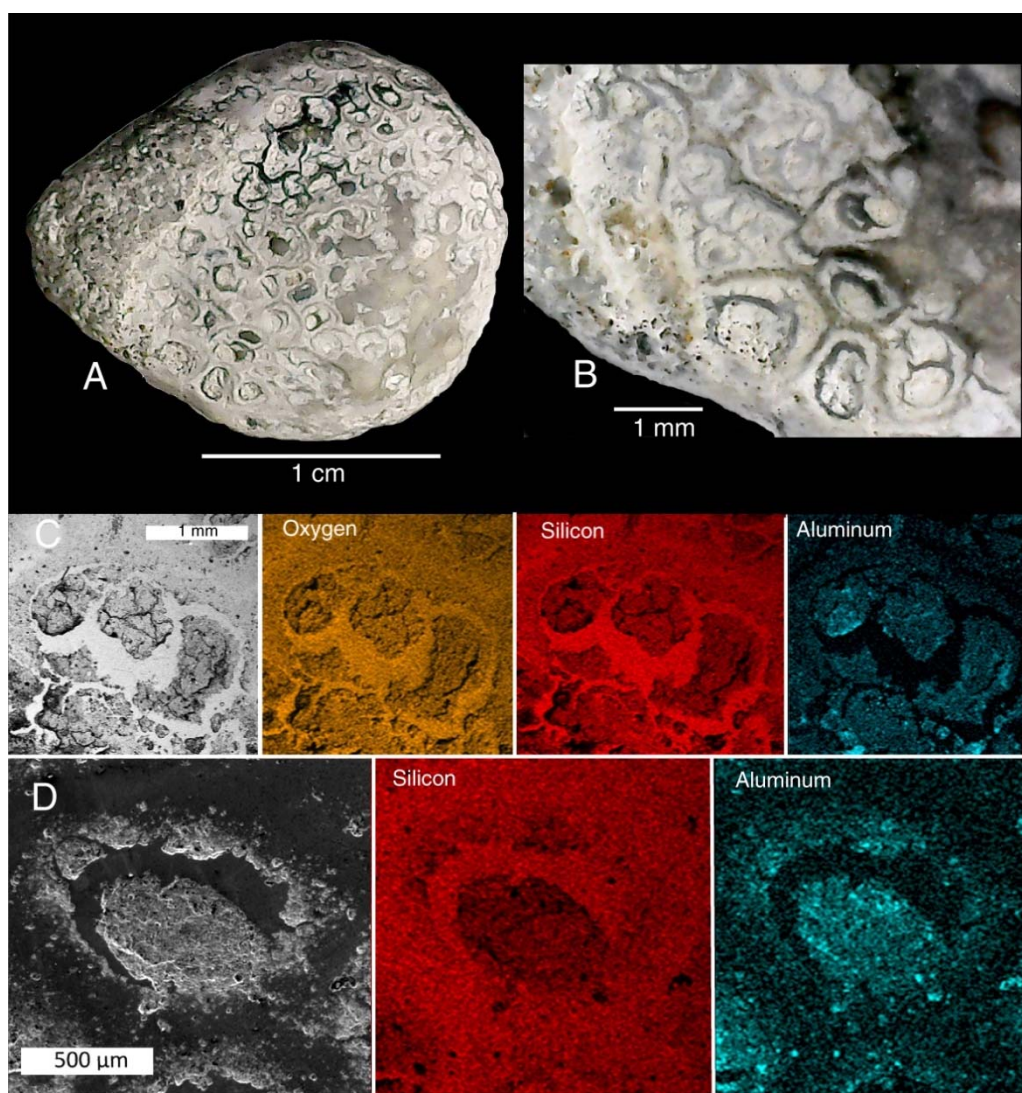


**Figure 24.** Water-worn opalized dinosaur bone, possibly a vertebral fragment, showing pneumatic cell architecture. Specimen RM-23. (A) Polished surface. (B) Magnified view showing opalized cells with sediment fill. (C) SEM/EDS map showing the distribution of O, Si, and Al. Cell walls are replaced by opal; filled spaces are Al-rich, presumably representing clay. (D) A single cell shows opal filling a semi-circular fracture that was produced by the shrinkage of clay that filled the cell interior.

#### 9.4. Evidence from Ichnofossils

Trace fossils from Lightning Ridge opal fields include coprolites and invertebrate burrows that have not been studied or previously reported from this locality. We examined two examples of opalized coprolites that were initially assumed to be plant fossils. One morphotype is ellipsoidal or lens-shaped, with a slightly pointed and rounded end (Figure 25). This coprolite contains plant fragments and small carbonaceous inclusions (Figure 25D). The second type is an amphipolar spiral form (Figure 26).

These shapes are not taxonomically distinctive. Spiral coprolites have been reported for diverse vertebrate taxa [71]. The small size provides constraints on the producer, and small amphipolar spiral coprolites are produced by a range of primitive fishes, including recent and fossil dipterans (lungfish). Both coprolites contain relict plant matter, indicating producers that were primarily herbivores, which is interesting because herbivore coprolites are generally less common in the fossil record than those of carnivores [72].

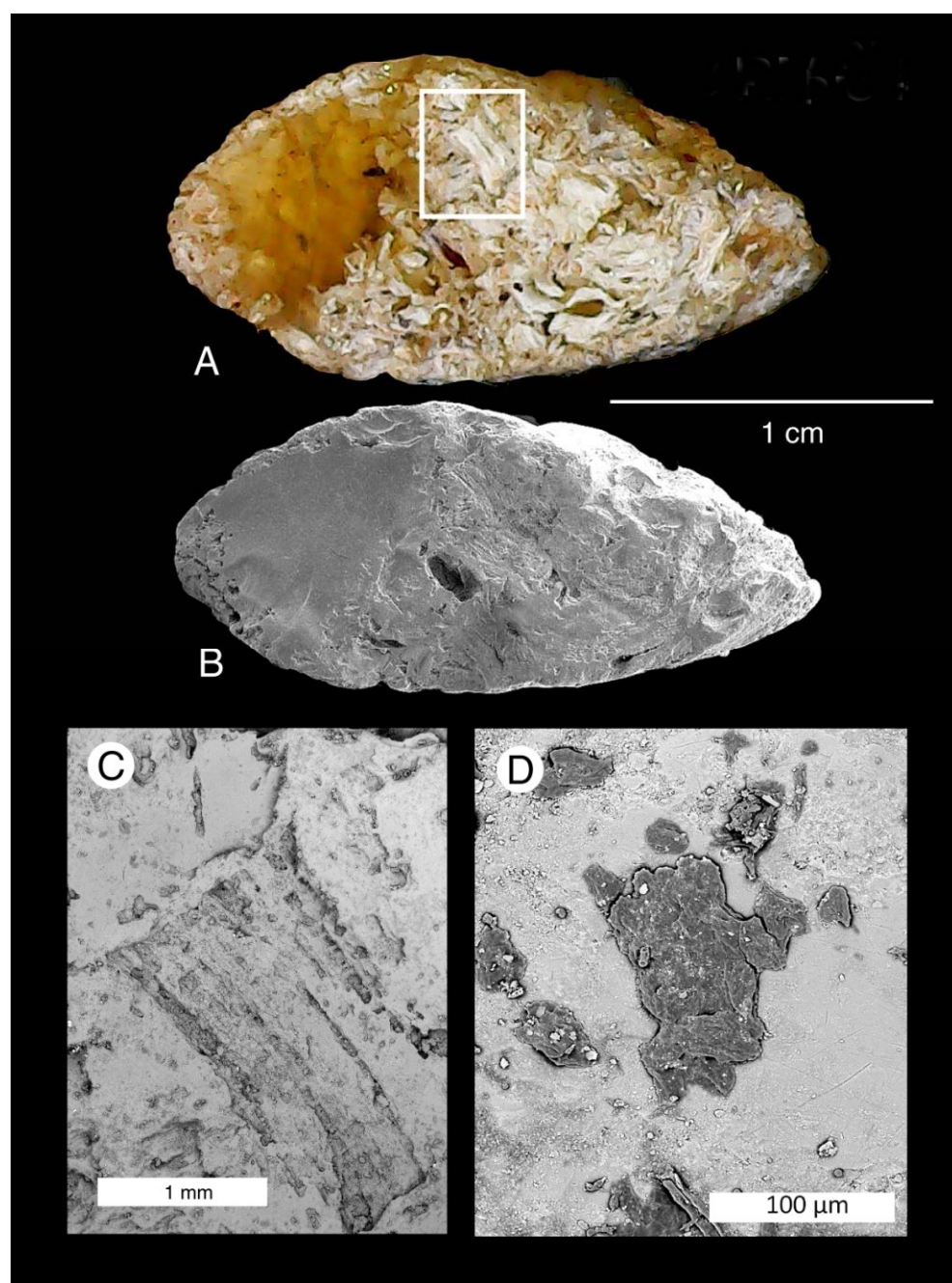


**Figure 25.** Coprolite Specimen RM-34. (A) Overall view. (B–D) SEM BSE images. (C) Included plant fragment showing fibrous structure, from outlined area in image A. (D) Carbonaceous inclusions in the silica matrix.

The spiral coprolite (Figure 26) is an excremental form characteristic of fishes [71]. Like many Lightning Ridge fossils, the specimen contains inclusions that have the “hollow box” structure, in which the original material has decomposed (Figure 25). The cut and polished surface reveals that the opal locally displays POC. Some inclusions contain remnants of silicified plant tissue (Figure 25E,F), indicating that the producer was a herbivore or omnivore. The abundance of silt-size sediment clasts (Figure 26G) suggests a substrate-grazing feeding style.

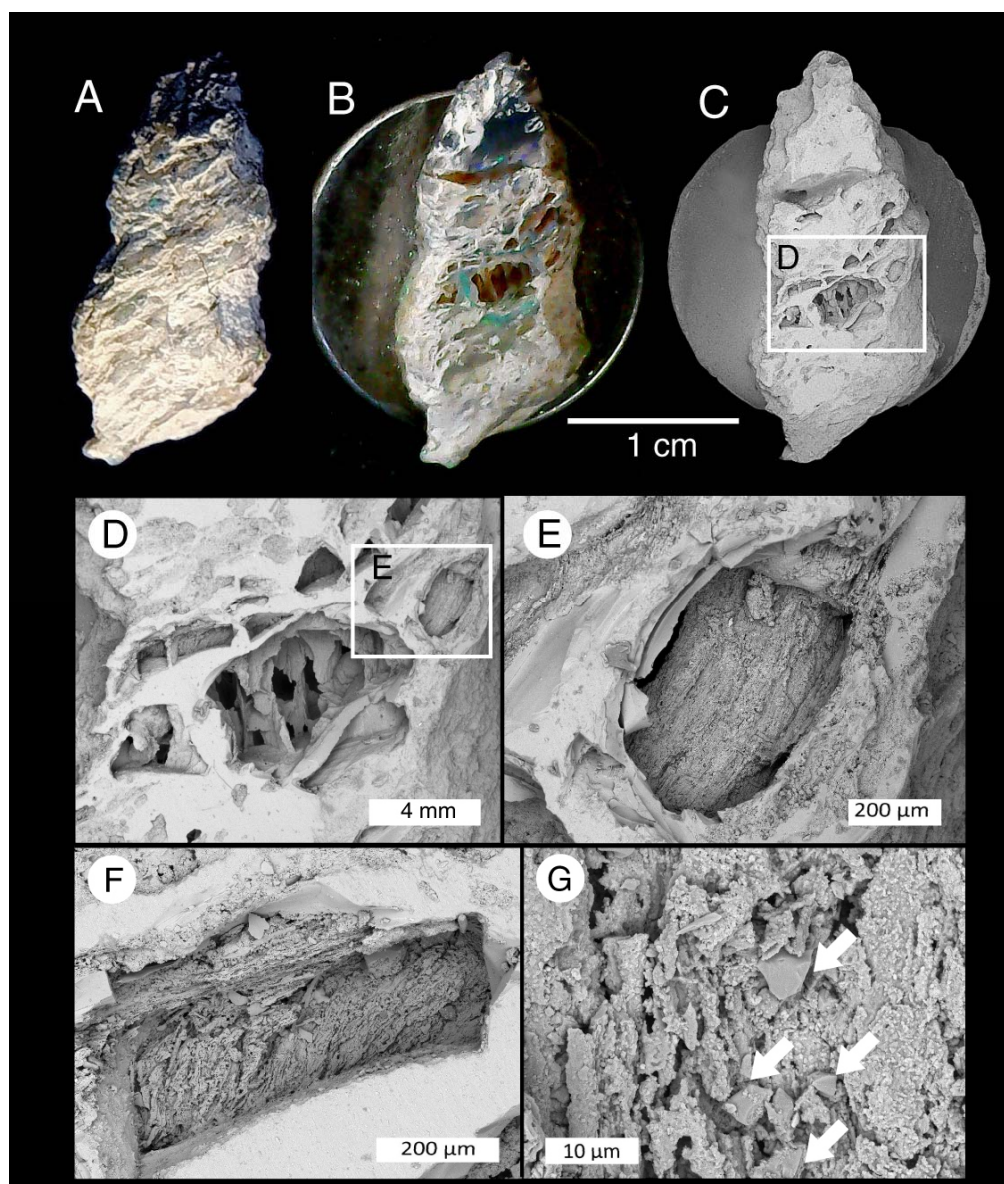


**Figure 26.** Spiral coprolite RM-33. (A) Specimen as originally collected. (B) SEM mount showing polished surface after grinding to reveal internal inclusions. (C) SEM BSE image showing cavities produced by the degradation of organic matter. Rectangle shows an ovoid inclusion that contains silicified plant tissue. (D) Cavity preserving surface texture of a wood fragment. (E) Enlargement of inclusion showing fibrous organic matter bounded by a thin, vitreous opal border. (F) A smaller inclusion preserving opalized plant tissue. (G) Higher-magnification image of degraded (partially digested?) plant tissue reveals abundant angular mineral grains.

Vertical burrow casts (*Ichnogenus Skolithos*) are common trace fossils at Lightning Ridge. They form short irregular tubes with diameters of 0.5–1 cm and lack internal septa or structural divisions. Shapes are variable, from simple or weakly tapered cylinders with rounded terminations (Figure 27A–D). Branched forms (Figure 27E–F) have a different origin, possibly representing casts of small roots or rhizoliths. Surface textures of both forms are commonly nodular. These ichnofossils are typically filled with white, gray, or translucent pectin; less commonly, the filling consists of precious opal.

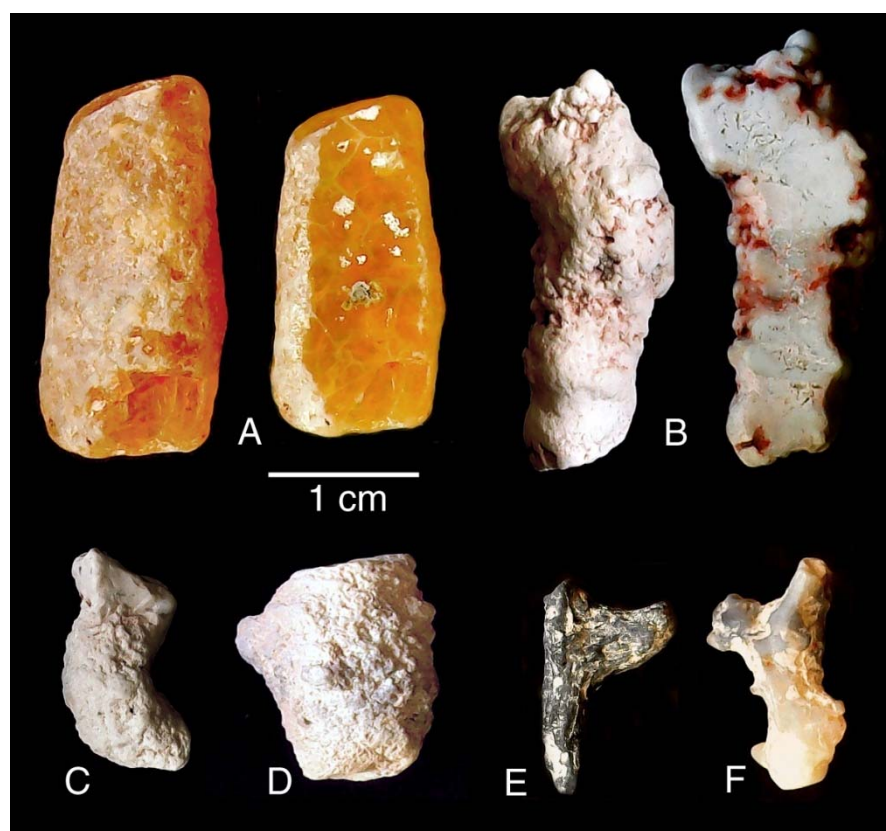


**Figure 27.** Trace fossils from the Lightning Ridge opal levels. (A) Short, cylindrical tube filled with translucent amber potch. Polished internal view (at right) shows a few microinclusions of claystone. Specimen GM-34A. (B) White, opaque “crockery potch” fills this curving tube, which has a botryoidal surface texture. The photo on the right shows the polished internal image. Specimen RM-50. (C) Curved burrow mineralized with potch. Specimen GM-32. (D) Burrow with rough wall texture. Specimen RM-49. (E,F) Narrow forms showing branched morphology. Specimens GM-33.

The nomenclature for trace fossils is based on morphology, without regard for the trace maker. *Skolithos*, characterized by vertical cylindrical burrows, has a geologic range from the Early Cambrian to the Recent, reported from marine and continental deposits. The diversity of these occurrences is evidence that these traces were made by a variety of organisms. At Lightning Ridge, the burrows often extend between the Finch Claystone sediments and the overlying steel band layer, and they may have provided conduits for the transport of silica-bearing fluids. Some specimens contain coarse sandy sediment similar to the fluvial materials of the steel band zone. The common taphonomic correlation of *Skolithos*, opalized plant remains, and mussel shells suggests that the vertical burrows may have been produced by polychaete worms that flourished in an environment dominated by the decay/decomposition of biomass. As with other Lightning Ridge fossils, the opalization of traces that were either empty or filled with porous sediment may have been a delayed process.

#### 10. Non-Opal Silicification

Plant materials in the Finch Claystone are mineralized with Opal-AG, but fossil wood from other positions in the sediment stack mineralized very differently. Figure 28 shows images of wood specimens from Early Cretaceous–Cenomanian Wallangulla Sandstone and from the Cenozoic Cumborah Gravel. In both formations, the wood is mineralized with microcrystalline quartz, as evidenced by bright birefringence in polarized light. This quartz mineralization presumably occurred at times when dissolved Si levels were relatively low, allowing orderly lattices to develop [73].

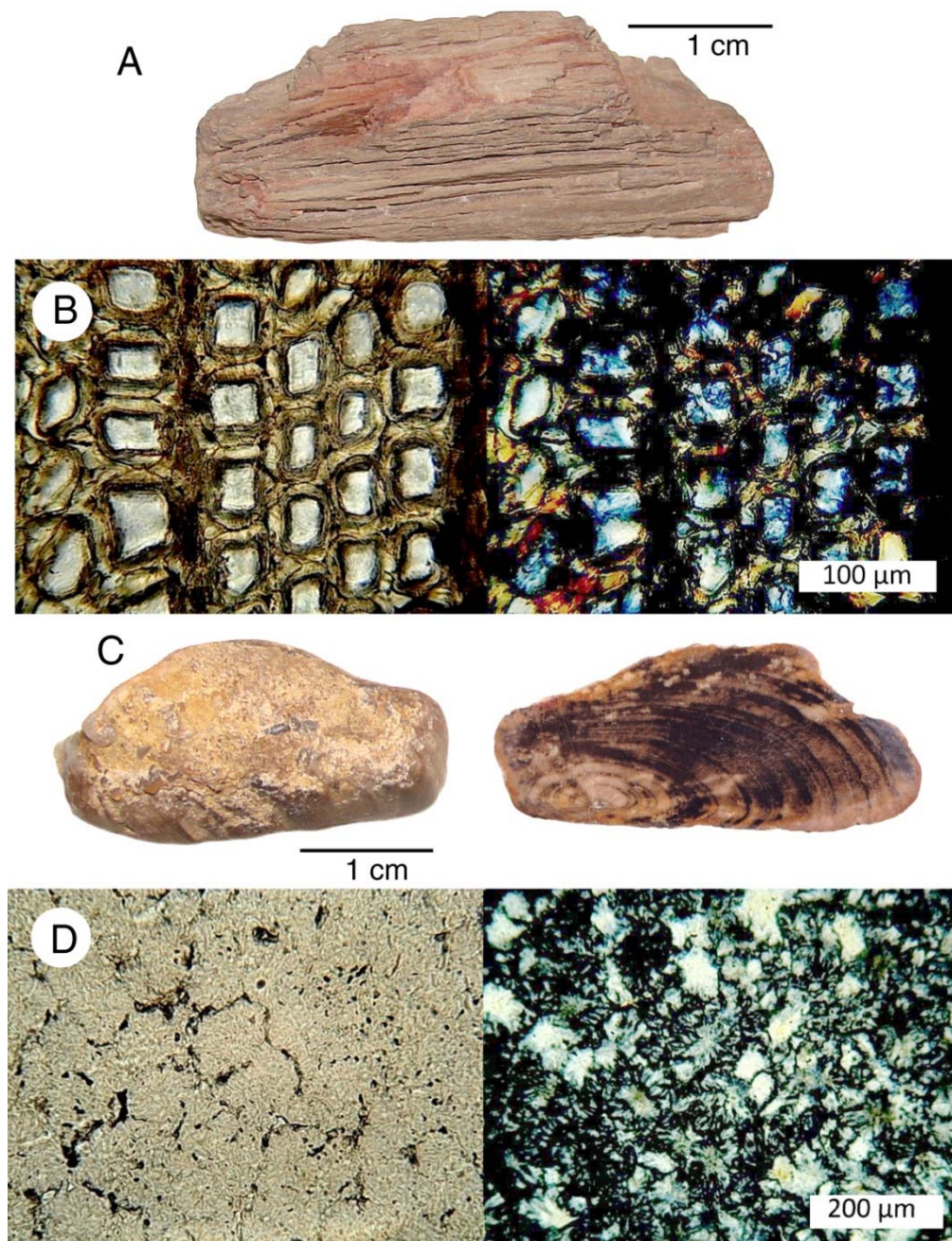


**Figure 28.** Quartz-mineralized wood from Lightning Ridge formations in strata that do not contain opal. (A) Petrified wood from lower Upper Cretaceous (Cenomanian) Wallangulla Sandstone. Specimen RM-14. (B) Thin-section transverse views: ordinary transmitted light illumination on the left photo, polarized light view on the right. Two stages of silica deposition are recorded: the silicification of cell walls, followed by silica deposition in the cell lumen. (C) Petrified wood from the Cenozoic Cumborah Gravel, Specimen RM-17. Images show the original surface on the left and a sawn and polished surface with annual growth ring patterns. (D) Thin-section views showing transverse orientation. Ordinary transmitted light illumination (photo on the left) shows poor anatomical preservation. Polarized light image (photo on the right) shows quartz that appears to have undergone diagenetic recrystallization.

### 11. Evidence from Other Opal Localities

Opal from the GAB has long been considered the product of a unique geologic setting, e.g., the statement by Rey [8]: “The formation of precious opal in the GAB can only be the fortuitous result of a set of geological circumstances perhaps unique on

Earth". However, opalization is a process that is widespread in the geologic record. Numerous localities produce precious opal. Opal-AG occurs in many sedimentary and geothermal environments. None are exactly analogous to Australian conditions, but in every instance, the formation and subsequent diagenesis of opal follows the basic principles of thermodynamics and geochemistry. For this reason, we have expanded our paleontological observations by considering occurrences of opal in a variety of geologic settings outside Australia.

### 11.1. European Opal Deposits

Curtis et al. [20] showed Australian localities as the only occurrences of Opal-AG in Cretaceous host strata, and the extensive opal occurrence list in that publication shows Opal-AG localities only at Dubnik, Slovakia, and Girona, Catalonia, both of which are Miocene in age.

The Slovakia and Catalonia localities lack a close geologic correspondence to Australian opal deposits. Dubnik opal is associated with volcanic flows and volcaniclastic rocks, in a hydrothermally altered surface zone. This precious opal is a mixture of "milk opal" and "glass opal" (hyalite, Opal-AN) [74]. Catalonia opal [75] consists of opaque masses of Opal-AG (commonly intermixed with Opal-CT), whose nodular shapes are referred to by collectors as "opal ninots" (opal dolls). They are informally named "menilite", a name originally ascribed to nodular opal from Oligocene strata in France [76]; similar forms also occur in the Neogene lacustrine sediments in the Carpathian region of Central Europe [77]. Although this is a morphotype not found in Australian opal deposits, without exception, European nodules containing Opal-AG occur in Neogene strata.

### 11.2. Evidence from Silicified Wood

The abundant presence of silicified wood in deposits that range in age from Paleozoic to Recent provides a perspective on rates for the transformation of opal to crystalline forms of silica. The most obvious trend is the preponderance of "agatized" wood in Mesozoic and Paleozoic fossil forests, where woods are mineralized with chalcedony or quartz. In contrast, opalized wood is abundant in Cenozoic locations, and in these deposits, wood mineralized with Opal-AG is relatively rare and seemingly limited to Neogene deposits.

### 11.3. Cenozoic Opal from Nevada, USA

Cenozoic localities in Nevada, USA, provide much closer models for the formation of sedimentary opal than the European occurrences. Opalized woods occur at various locations in northern and central Nevada, where extensive Cenozoic volcanism produced abundant felsic lavas and associated pyroclastics and tephra, which all provided potential sources of dissolved silica [78]. The mild, humid Cenozoic climate allowed forests to flourish in a region that is now arid. The collapse of calderas led to the development of lakes; fossil wood typically represents driftwood that accumulated along the ancient shorelines. The compositions of Cenozoic fossil woods at these Nevada localities show a correspondence to age. Pliocene fossil wood at Lyon County in central Nevada is mineralized only with Opal-AG. Woods from Oligocene and Eocene locations are characteristically mineralized with chalcedony or quartz, not opal (Figure 29). Miocene fossil wood provides the best opportunities for observing the deposition of sedimentary opal and subsequent diagenetic changes.

We focus on the opal-bearing late Miocene strata of the Virgin Valley Formation in northern Humboldt County, Nevada, USA, where prospecting and opal mining began in earnest in 1907 and several of the largest mines have been in continuous production for more than a century.

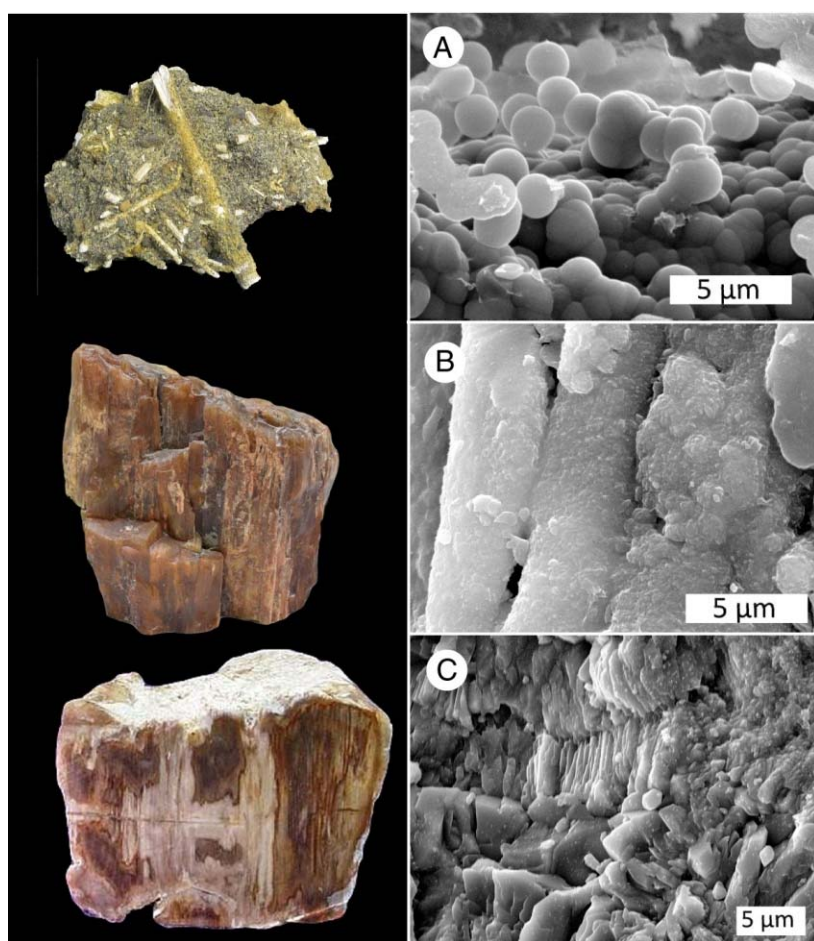


**Figure 29.** Silicified Cenozoic wood of varying mineral compositions from Nevada, USA. (A) Opal-AG. Hazen, Churchill County, Pliocene. Disordered lepispheres are visible in the SEM image. (B) Quartz-mineralized wood, Badger Flat, Humboldt County. The SEM image shows relict Opal-AG lepispheres. (C) Quartz-mineralized wood from Devil's Gate, Elko County. The SE image reveals the columnar structure of chalcedony.

Virgin Valley precious opal has spectacular play of color, and even small specimens sell for high prices. A gemological limitation is that some opal specimens are prone to developing cracks from dehydration; mined specimens are usually stored in vials of water prior to sale. This stability issue was discussed in detail by Chauviré et al. [79]. Although they do not form the very precise geometric lattices seen in Opal-AG from Australia, where precious Opal-CT occurs only in volcanic geologic settings [80], microspheres in Virgin Valley Opal-CT are sufficiently ordered to cause light dispersion (Figure 30). Despite these contrasts, it is not unusual to observe the presence of Opal-AG when non-precious Virgin Valley specimens are examined by SEM.

Virgin Valley, Nevada, shares some geologic similarities to opal deposits of the Great Artesian Basin in Australia. Both regions are now arid and alkaline, but deposition was during a time of a milder, wetter climate. Sedimentation occurred in or near inland water bodies, with volcanoclastic debris being a major component of the sediment. A significant difference is that plant fossils in Virgin Valley consist of mineralized tissue, in contrast to the Australian preservation of fossils only as casts. Further, as previously noted, the Virgin Valley specimens consist of Opal-CT and Opal-AG, with play of color associated only with Opal-CT, a pronounced contrast to the exclusively Opal-AG composition of Australian sedimentary opals.

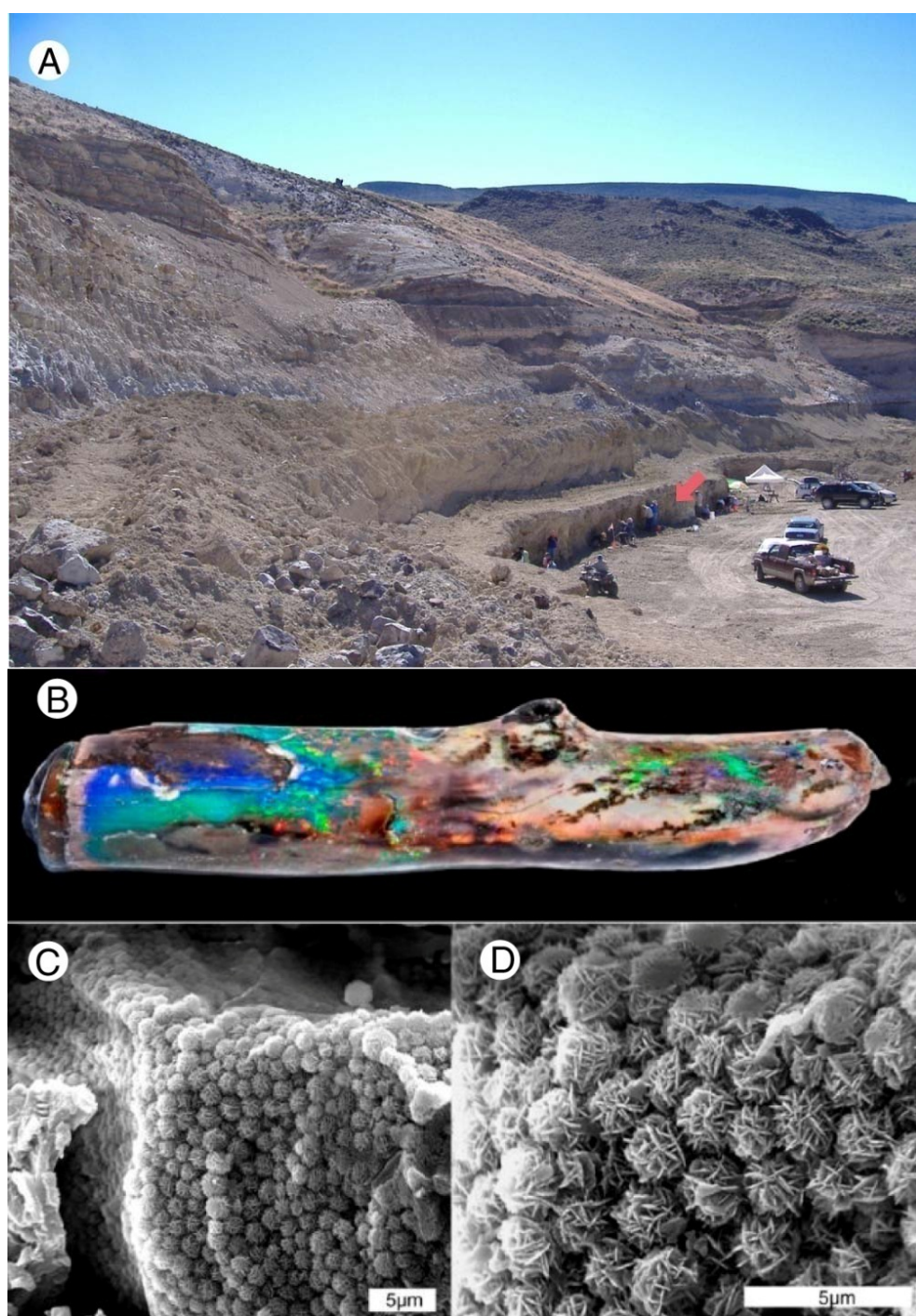


**Figure 30.** Precious opal from the Virgin Valley mining district, northern Nevada, USA. (A) Open-slope mining at the Royal Peacock Mine. The opal-bearing stratum is shown with a red arrow. (B) Opalized limb from the Royal Peacock Mine. (C,D) SEM images of Virgin Valley precious opal with well-ordered Opal-CT.

Another difference is that most Virgin Valley precious opal occurs only as mineralized wood. The deposit lacks the occurrence of nobby and seam opal that are the major sources of opal at Lightning Ridge. The Virgin Valley Formation does not have well-defined silicified clastic strata kin to the steel band unit at Lightning Ridge. Instead, the formation includes diatomite that in places has been altered to form thick, continuous layers of common opal. The Virgin Valley basin does not have a regionally prominent artesian hydrology, but upwelling hot springs are locally present.

Some of the wood is entirely mineralized by Opal-AG, always in the form of potch. Other specimens contain both Opal-AG and Opal-CT, including examples that appear to show evidence of transformation. Many specimens contain only Opal-CT (Figure 31). A single stratum may yield specimens that have a multiplicity of compositions, which suggest that the geochemical gradients were highly localized.

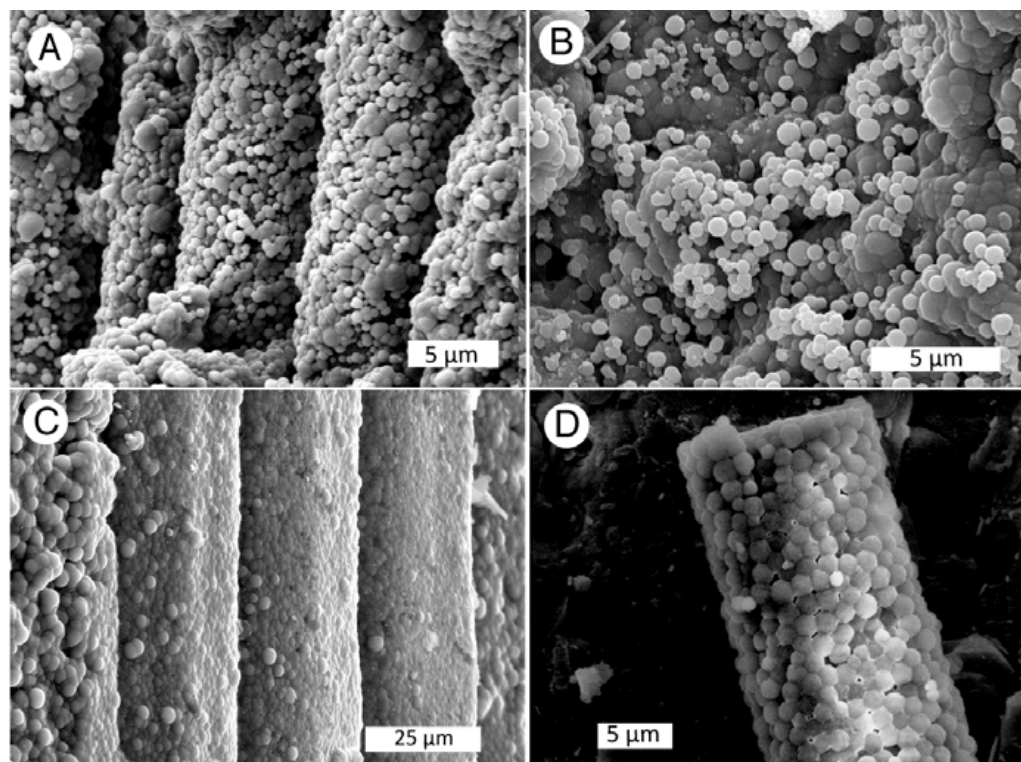


**Figure 31.** SEM images show that some upper Miocene woods from the Virgin Valley, Nevada, USA opal mining district contain Opal-AG, always in the form of potch. (A) Longitudinal view of adjacent cells that have been replaced by Opal-AG lepispheres. Specimen from the Section 27 opal claim. (B) Scattered Opal-AG lepispheres on opalized wood, also from the Section 27 opal claim. (C,D) Longitudinal view of wood cells replaced by Opal-AG, Washoe Valley.

Lepisphere sizes are relatively large in Nevada opal, making them readily visible in SEM images. A general absence of silica cement means that lepispheres of both Opal-AG and Opal-CT are commonly discernable without requiring HF etching. Opal-AG occurs in three morphotypes. In some samples, the opal occurs as a multitude of individual spheres (Figure 30).

In other specimens, Opal-AG occurs in a botryoidal form, and as porous, crinkly masses (Figure 31). In all instances, the amorphous composition of Opal-AG is evidenced by the absence of birefringence under polarized light, and the lack of distinctive peaks in X-ray diffraction patterns [78].

Specimens of opalized wood in the Virgin Valley Formation commonly show a complex mineralogic structure (Figure 32). These compositions provide evidence that silica deposition occurred in several discrete episodes, typically beginning with the permineralization (and eventual replacement) of cell walls, followed by subsequent silica precipitation in the cell lumen and intercellular spaces [78].

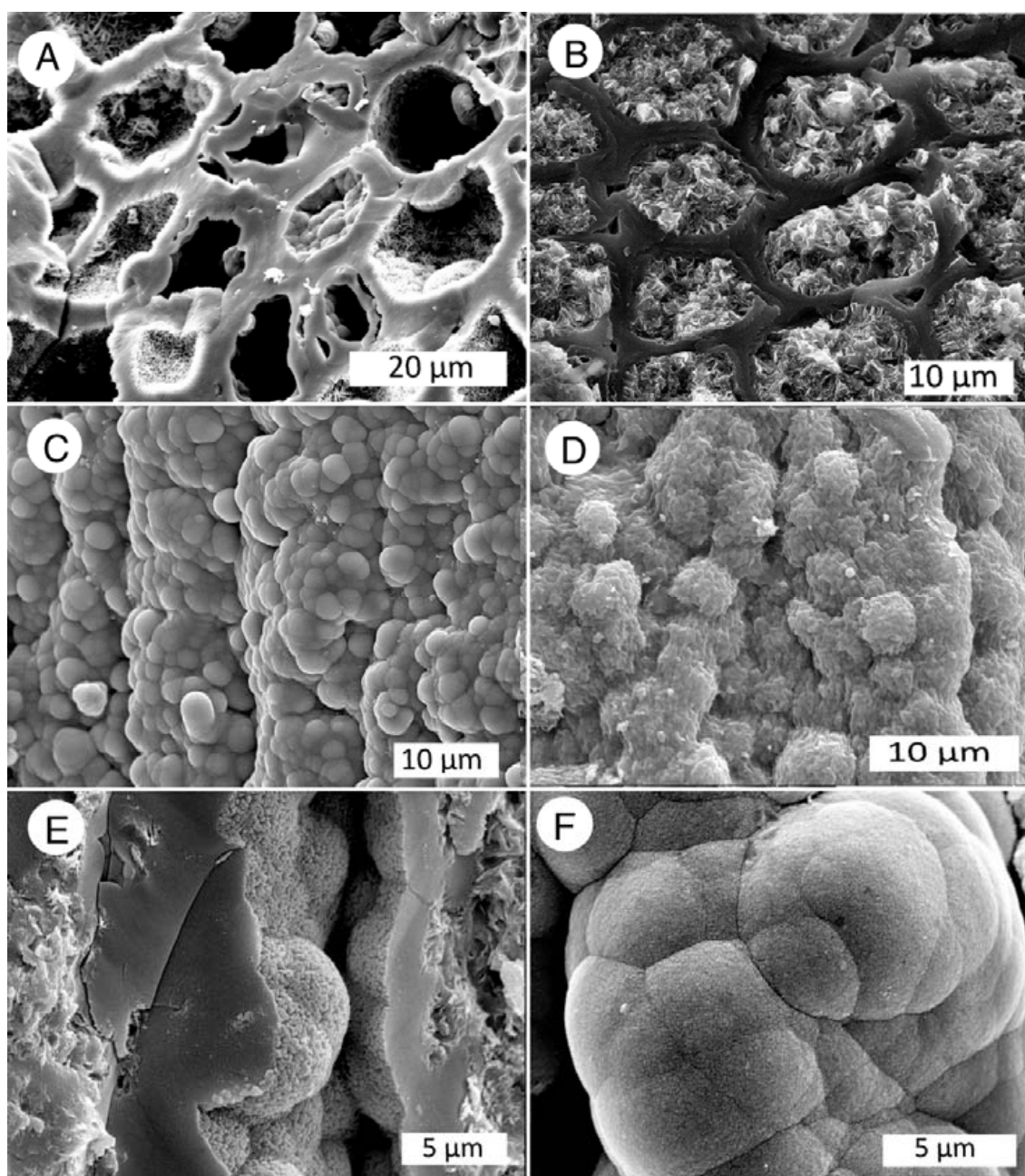


**Figure 32.** Opal-AG and mixed Opal-AG/Opal-CT morphologies in Miocene fossil woods from the Virgin Valley opal mining district, Nevada, USA. (A) Transverse view of wood in which some cells contain incipient Opal-CT coatings, Cessilly Ann Claim. (B) Wood that has cell walls replaced by vitreous Opal-AG, with lumen filled with porous Opal-AG, Toni Claim. (C) Wood mineralized with botryoidal Opal-AG, Royal Peacock Mine. (D) Silicified wood composed of microcrystalline quartz that appears to mimic the original botryoidal morphology, Badger Flat. (E,F) Botryoidal opal, where vitreous masses appear to be developing the incipient crystallinity of Opal-CT, Rainbow Ridge Mine.

Fossil wood in the Virgin Valley Formation commonly contains abundant Opal-CT, locally in association with other materials but often present as the major constituent (Figure 33).

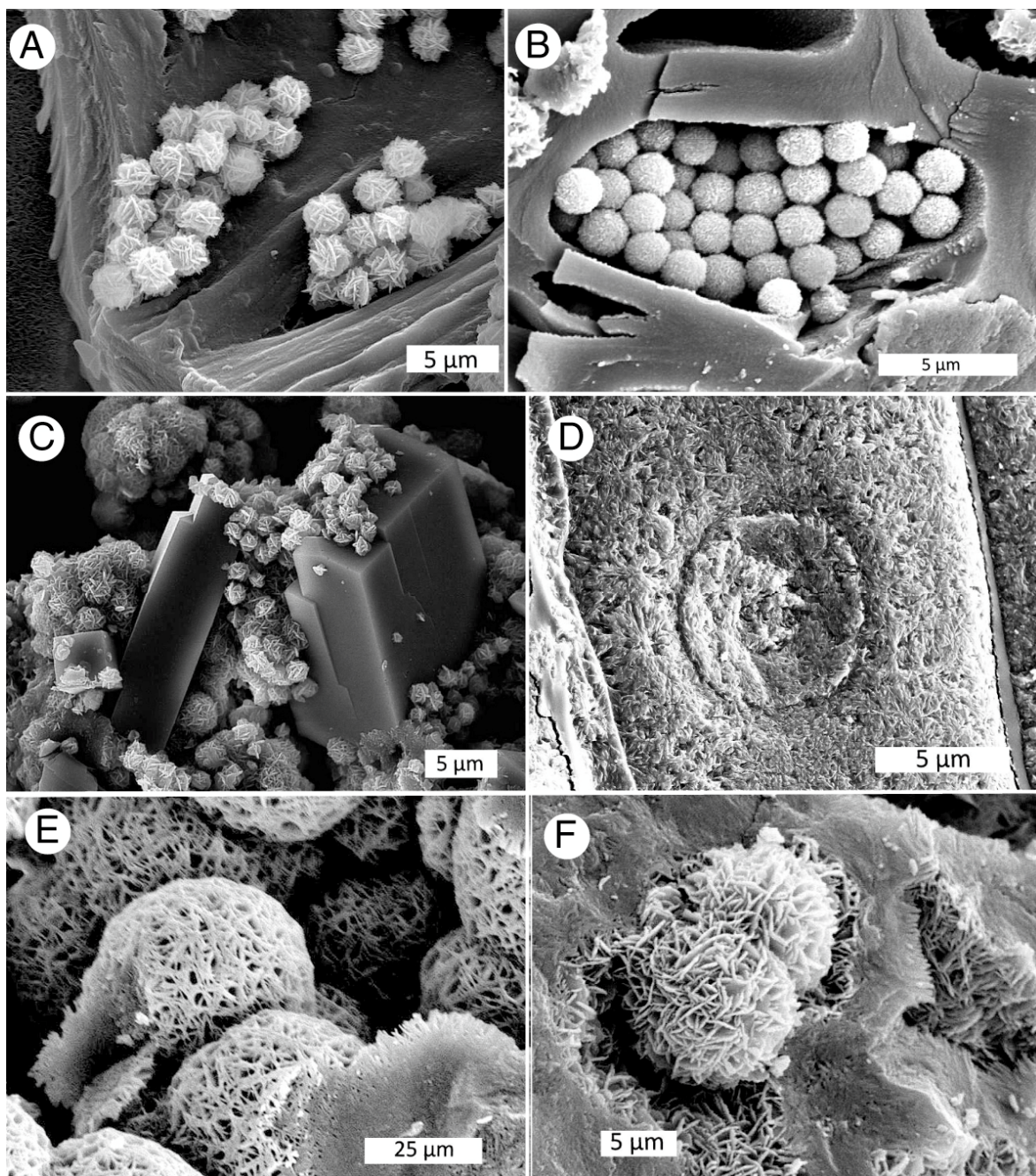


**Figure 33.** SEM images of Virgin Valley specimens that contain Opal-CT as the primary form of silica. (A,B) Opal-CT lepispheres in cells of carbonized wood, Royal Peacock Mine. (C) Opal-CT lepispheres on zeolite crystals, Rainbow Ridge Mine. Zeolite crystals result from the alteration of volcanic ash in the lacustrine sediment that encloses the fossil wood. (D) A single tracheid showing an internal cast of an intervessel pit, the tissue replaced by Opal-CT. Washoe Valley. (E,F) Opal-CT lepispheres, Pandora Mine.

## 12. Opal Diagenesis

Relatively rapid transformations of Opal-A to Opal-CT are well-documented for silica minerals in siliceous sinters and sediments that contain biogenic silica. In those geologic environments, Opal-A alters to Opal-CT, which in turn transforms to quartz. The diagenetic transformation sequence has been described in detail by Liesegang and Tomaschek [81].

### 12.1. Biogenic Silica

The occurrence of Opal-AG in young deposits suggests that this material may transform to Opal-CT at a rapid rate. Transformation of Opal-AG to crystalline silica has been reported for Cenozoic diatomite [82–89] and confirmed in laboratory experiments [90,91]. Temporal distributions of silica polymorphs are shown in Figures 34 and 35.

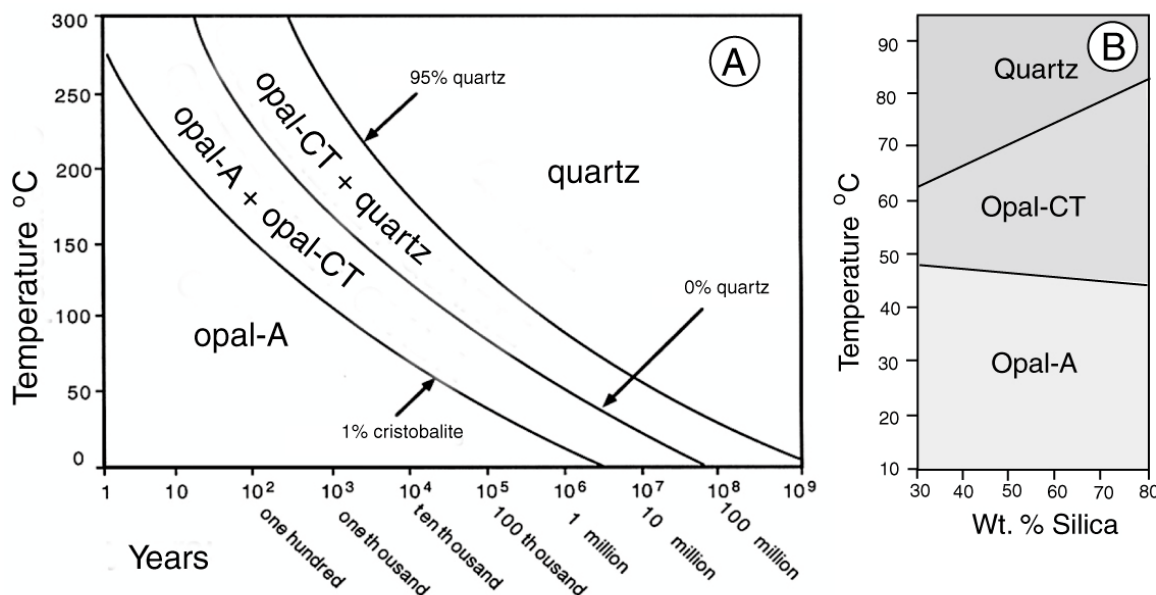


**Figure 34.** Generalized stability fields for opal and quartz. (A) Mitzutani [84] based his diagram on field observations and experimental studies, estimating ages required for silica-phase transformations. (B) The Behl et al. plot [92] is based on the % of silica in biogenic sediments versus burial temperature. Highly elevated temperatures are not required for the transformation of Opal-A to Opal-CT.

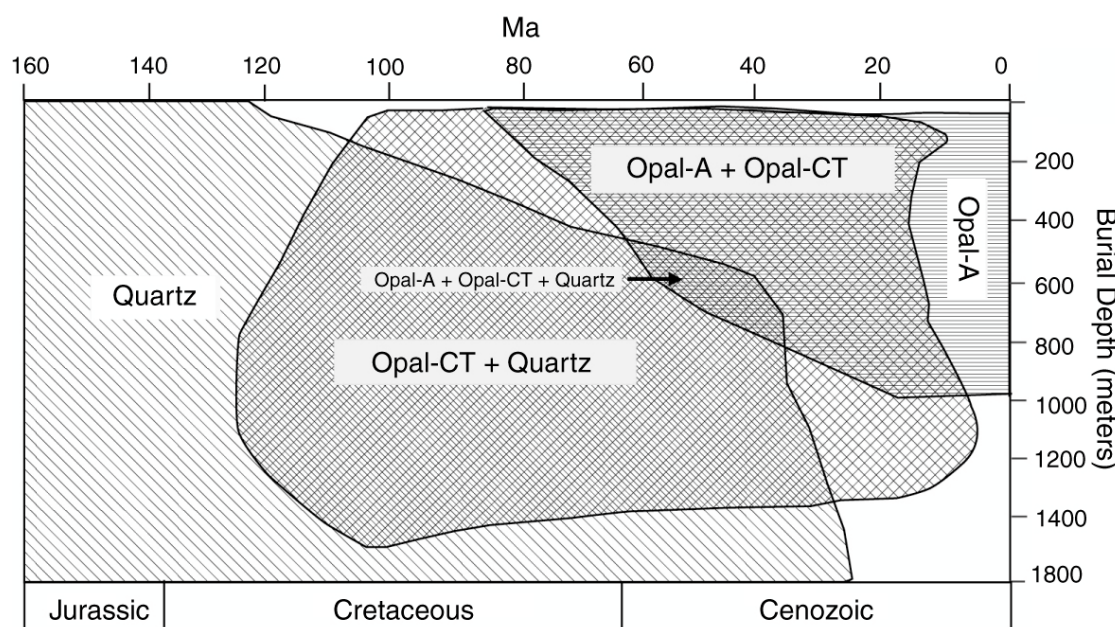


**Figure 35.** Worldwide distribution of silica polymorphs in deep sea sediments graphed with respect to geologic age. Graph adapted from Hesse [93]. Pure Opal-A was only found in young Cenozoic sediments. Diagenetic transformations of opal to quartz were inferred to be relatively slow. The broad Opal-CT + quartz zone contrasts to continental deposits, where opal is generally absent in Mesozoic sedimentary environments. Perhaps reaction rates are very different for deep seafloor environments.

## 12.2. Silica Sinter

Estimates based on siliceous sinter provide additional evidence of rapid silica transformation. Siliceous sinter is initially precipitated as Opal-A, changing with time to other forms of silica [94,95]. Herdianita et al. [94] reported that Opal-A remains relatively unchanged for ~10,000 years. Between 10,000 and 50,000 years, the sinter transforms to Opal-C or Opal-CT; after ~50,000 years, microcrystalline quartz becomes the dominant constituent. Lynne et al. [95] observed that at Roosevelt Hot Springs, Utah, USA, the transformation of amorphous silica to Opal-CT and then to quartz occurred within 1900 years.

In natural environments, silica transformations may be affected by a variety of factors, including the presence of detrital minerals [96]. Transformation rates may be greatly accelerated in the presence of sulfur, calcite, alunite, or plant remains. For example, dissolved magnesium may accelerate the transformation because colloidal magnesium hydroxide serves as a nucleus for Opal-CT crystallization [97,98]. Under some sedimentary conditions, Opal-A may transform directly to quartz, without an Opal-CT intermediate stage [96].

As an additional complexity for the diagenesis hypothesis, the transition of Opal-A to Opal-CT may not be the only explanation for the existence of these polymorphs. Both polymorphs occur in a palygorskite clay deposit in China, but Opal-CT is not a crystallization product of Opal-A. Opal-A precipitates during times of dry climate where groundwater input is low. Opal-CT precipitates during periods of humid climate when groundwater input is high [99].

## 13. Discussion

Our research reveals that Lightning Ridge fossils show evidence for delayed opalization. Fine, clay-rich sediment provided a high-fidelity molding material for preserving organic shapes and obstructed decomposition over a protracted period. This is true for plants, invertebrates and vertebrates, and trace fossils (e.g., coprolites). In the case of vertebrate bone specimens, the internal microstructure is variably preserved with no trace of biomineral.

The timing of opal precipitation is not discernable from fossil evidence, but various other characteristics of the Lightning Ridge opal deposits suggest that opalization was a Neogene phenomenon.

The opalization of faults and fractures is suggested to be related to intermittent Miocene tectonism. The cross-cutting relationships of opal veins or seams are evidence that opal was precipitated in multiple episodes, which is consistent with opal features that we observed in fossils (e.g., Figure 11). We also emphasize that faults and fractures, and sporadic cases of opalization, could have resulted from the expansion and contraction of hydroplastic sediments subject to sporadic and variable climatic events.

A relatively young age for opal precipitation is supported by the occurrence of Opal-AG and Opal-CT in other locations. Opal-AG is a metastable material that rapidly transforms to Opal-CT and later to cryptocrystalline or microcrystalline quartz, even under conditions of relatively low temperature and burial depth. Worldwide, Opal-AG is limited to Neogene deposits, with occurrences that include siliceous biogenic sediments, geothermal sinters, and silicified wood. In deposits older than the Pliocene, Opal-AG typically occurs in association with Opal-CT, implying mineralogic transformation.

Information from fossils does not provide a predictive device for understanding the processes that lead to opal precipitation in “spot” locations in the field. The stratigraphic and sedimentologic characteristics support the concept that silicification was controlled by pH and eH gradients at the contact zone between alkaline and acidic groundwater, and fossil evidence does not conflict with the deep weathering [6] and mound springs [30–32] hypotheses. Evidence from fossils does provide constraints for some of the other models that have been proposed.

The phenomenon of delayed mineralization and the low “shelf life” of Opal-AG support a Cenozoic (probably Neogene) age for opal formation and evidence of multiple

episodes of silica precipitation supports models for polygenetic processes (e.g., syntectonic mechanisms [16–24]).

In particular, information from fossils constrains the timing of opal formation. Mineralogical evidence conflicts with interpretations that infer Cretaceous opal formation (e.g., [8,30,31]). The data are also contrary to models that invoke a modern age for opal formation [34,35]. The purported 1000–7000 BP ages published by Dowell et al. [34] do not meet the accepted standards for radiometric data reporting. The briefly-described results provided no indication of the number of samples that were analyzed or the standard deviation of the data. Analyses were reported to have been performed “using the mass spectrometer at the Research School of Physics (RSPhys), Australian National University”, but it was not established that the facility was accredited for radiocarbon analysis. Rey [8] has discussed the potential for dating error caused by the porosity of opal, which allows contamination from young microbes or other sources of extraneous young carbon.

The premise that opal precipitation was generally related to microbial productivity is likewise questionable. The theory [30,31] proposes that microbial opal precipitation occurred during the Cretaceous, which conflicts outright with the thermodynamic instability of amorphous opal. The microbial model is also at variance with studies of biomimetic mineralization that indicate a need for large microbial populations and high nutrient levels [100]. Additionally, at high magnifications, Lightning Ridge opal textures are inconsistent with the distinctive microbial textures observed at sites where silica biomimetic mineralization is well documented [101,102]. Although it might be expected that during breakdown of organic matter, microbes would be omnipresent, in our own SEM studies of opalized fossils, no relict microbes were observed. Although fossil microbes may be present in some specimens, they are not a universal characteristic in Lightning Ridge opal.

Lightning Ridge specimens are excavated under a range of conditions in which the potential for modern microbial contamination is formidable and Deveson’s ability to culture living microbes from the opal clays [35] is not surprising, given the ubiquity of bacteria and fungi in everyday environments.

A key element of our findings is that plant, invertebrate, and vertebrate remains all show evidence of delayed mineralization. Early Cretaceous organisms were buried in clay-rich sediment and the eventual decomposition of the organic matter produced molds that later became sites for opal precipitation. The timing of this opalization is not determinable from fossils, but the diagenetic history in worldwide locations suggests that the Opal-AG composition is evidence of Neogene mineralization.

This delayed mineralization likely resulted from several factors. The degradation of cellulosic material in wood, calcium carbonate in mollusks, and bioapatite in bones are processes dependent on pH, Eh, temperature, and elemental availability, which have no direct relationship to burial duration. The subsequent entry of opal into mold spaces depends on the consistency of the enclosing clay and the ability of silica-bearing fluids to permeate the spaces. This fluid migration may have been related to folding, faulting, and fracturing from Neogene tectonic activity.

#### 14. Conclusions

There is a general consensus about the basic geologic aspects of opal precipitation in the Great Artesian Basin. The principal host rocks were organic-rich volcaniclastic sediments deposited from ~122–91 Ma when Central Australia was inundated by a shallow epicontinental sea. As marine influences receded, fluvial sediments became increasingly abundant, resulting in a stratigraphic sequence that is lithologically diverse, including thick sandstones and intervening claystone. The precipitation of opal involved the dissolution of silica from felsic source beds under conditions of alkaline pH and the development of a geochemical gradient where silica-bearing groundwater interacted with acidic water to yield colloidal silica as a source material for Opal-AG.

The enigma is the timing of this opalization. Evidence from Lightning Ridge fossils shows that the silification of organic remains and emplacement of opal was a delayed

process, occurring only after the time required for the decomposition of the original organic material. This delayed mineralization was observed in plant, invertebrate, and vertebrate fossils. The causes of this delay may have involved paleohydrologic and paleoclimatic factors, along with geologic events. Horton [103] noted the potential importance of increased aridity beginning at ~40 Ma (Late Eocene) as a trigger for opalization, a time when the lowering of the water table was accompanied by a rise in pH. Mild tectonism at ~24 Ma (Late Oligocene) created gentle folds that facilitated the lateral and vertical migration of silica-bearing solutions. Pecover [22–29] suggested that Miocene folding and faulting explains the structural geometry of opal-bearing fractures.

Evidence from opalized fossils and comparisons of opal diagenesis at international localities support hypotheses of a Neogene origin for opal at Lightning Ridge and presumably other opal localities in the Great Artesian Basin. Opal fossils described in this report reveal that opal was precipitated in multiple episodes, resulting from many factors. Our work does not contradict the detailed observations of other investigators, e.g., Rey [8], Hermann and Maas [12], and Pecover [22–28]. Our evidence documents the value of fossils for interpreting the origin of opal and provides constraints on the timing of opalization. We suggest that occurrences of opal in other locations are relevant to understanding the origin of Australian opal. Our work does not provide a definitive explanation; it is merely a step forward in what continues to be a long walkabout.

**Author Contributions:** Both authors participated in the design of the research and in the writing of the manuscript, and were involved with the interpretation of data. Laboratory analyses were performed by Mustoe using facilities at the Western Washington University, Bellingham, WA, USA. All authors have read and agreed to the published version of the manuscript.

**Funding:** This research involved no external funding.

**Data Availability Statement:** Many opal specimens used in this study are from the public collection of the Australia Opal Centre Ltd. P.O. Box 229, 3/11 Morilla St., Lightning Ridge, NSW, 2834 (<https://www.australianopalcentre.com>). Nevada fossil wood specimens are archived at the Geology Department, Western Washington University, Bellingham, WA 98225, USA (<https://geology.wwu.edu/>). More detailed information about these Nevada specimens can be found in [76].

**Acknowledgments:** Access to the analytical facilities at the Western Washington University was facilitated by Michael Kraft, University Instrument Center, and Kyle Mikkelsen, Advanced Materials Science and Engineering Center. Photographs by Robert A. Smith were used with his permission and with permission of the Australian Opal Centre, Lightning Ridge, Australia. Phil Bell provided the samples of ichthyosaur bone for analysis from his study area in the Griman Creek Formation, Bymont Station, Surat, Queensland. Donors under the Australian Government Cultural Gifts Program were Dave Barclay, Vicki Bokros, Peter Drackette, DTEO P/L, Jack Fahey, Mike Poben, Paul Sedawie, Steve Turner, and Clytie Smith. We thank four peer reviewers for their encouraging remarks. We acknowledge the Yuwaalaraay, Yuwaalayaay, and Gamilaraay custodians of the country in the Lightning Ridge district and pay our respects to Elders past, present and future.

**Conflicts of Interest:** The authors declare no conflict of interest.

## References

- Chauviré, B.; Robdeau, B.; Mazzero, F.; Ayalew, D. The precious opal deposit at Wegel Tena, Ethiopia: Formation via successive pedogenic events. *Can. Mineral.* **2017**, *55*, 707–723. [[CrossRef](#)]
- Rondeau, B.; Cenki-tx, B.; Fritsch, E.; Maxxero, F.; Beckele, E.; Gallou, E.; Ayalew, D.; Beckele, E.; Gaillou, E.; Ayalew, D. Geochemical and petrological characterization of gem opals from Wegel Tena, Welo, Ethiopia: Opal formation in soil. *Geochem. Explan. Environ. Anal.* **2012**, *49*, 827–836.
- Berger, B. Fossilized Insect Discovered Not in Amber, But in Opal. *EntomologyToday*, 18 January 2019. Available online: [https://entomologytoday.org/2019/01/18/fossilized-insect-discovered-amberopal/?fbclid=IwAR3tvq4p9ZxpCQ8qBNd29sRDsvWxLu\\_DpKqC9SgOwPgPvxuwFGVH8g3yBcQ#](https://entomologytoday.org/2019/01/18/fossilized-insect-discovered-amberopal/?fbclid=IwAR3tvq4p9ZxpCQ8qBNd29sRDsvWxLu_DpKqC9SgOwPgPvxuwFGVH8g3yBcQ#) (accessed on 12 September 2023).
- Coldham, T.; Ivey, J. A visit to the Indonesian opal fields in 2019—Opal types, mining and treatments, Part 1. *Aust. Gemmol.* **2020**, *27*, 199–213.
- Henderson, R.A.; Johnson, D. *The Geology of Australia*, 3rd ed.; Cambridge University Press: Cambridge, UK, 2016; p. 375.

6. Brown, D.A.; Capbell, K.S.W.; Crook, K.A.W. *Geological Evolution of Australia and New Zealand*; Pergamon Press: Oxford, UK, 1968; p. 409.
7. Bryan, S.E.; Constantine, A.E.; Stephens, C.J.; Ewart, A.; Schön, R.E.; Parianos, J. Early Cretaceous volcano-sedimentary successions along the eastern Australia continental margin: Implications for the break-up of eastern Gondwana. *Earth Planet. Sci. Lett.* **1997**, *153*, 85–102. [[CrossRef](#)]
8. Rey, P.F. Opalization of the Great Artesian Basin (central Australia): And Australia story with a Martian twist. *Aust. J. Earth Sci.* **2013**, *6*, 291–314. [[CrossRef](#)]
9. Bell, P.R.; Brougham, T.; Herne, M.C.; Frauenfelder, T.; Smith, E.T. *Fostoria dhimbangunmal*, gen. et sp. nov., a new iguanodontian (Dinosauria, Ornithopoda) from the mid-Cretaceous of Lightning Ridge, New South Wales, Australia. *J. Vertebr. Paleontol.* **2019**, *39*, e1564757. [[CrossRef](#)]
10. Bell, P.R.; Fanti, F.; Hart, L.J.; Milan, L.A.; Craven, S.J.; Brougham, T.; Smith, E. Revised geology, age and vertebrate diversity of the dinosaur-bearing Grimman Creek Formation (Cenomanian), Lightning Ridge, New South Wales, Australia. *Palaeogeogr. Palaeoclimatol. Palaeoecol.* **2019**, *514*, 31–182. [[CrossRef](#)]
11. Dutkiewicz, A.; Landgrebe, T.C.W.; Rey, P.F. Origin of silica and fingerprinting of Australian and sedimentary opals. *Gondwana Res.* **2015**, *27*, 785–795. [[CrossRef](#)]
12. Herrmann, J.; Maas, R. Formation of sediment-hosted Opal-A<sub>G</sub> at Lightning Ridge (New South Wales, Australia): Refining the deep-weathering model. *J. Geol.* **2022**, *130*, 77–109. [[CrossRef](#)]
13. Smith, E.; Smith, R. *Black Opal Fossils of Lightning Ridge*; Kangaroo Press: East Roseville, NSW, Australia, 1999; p. 112.
14. Smallwood, A.G. A new era for opal nomenclature. *Aust. Gemmol.* **1997**, *19*, 486–496.
15. Levin, I.; Ott, E. X-ray study of opals, silica glass and silica gel. *Z. Kristallogr.* **1933**, *85*, 305–318. [[CrossRef](#)]
16. Dwyer, F.O.; Mellor, D.P. An X-ray study of opals. *J. Proc. R. Soc. NSW* **1934**, *68*, 47–50. [[CrossRef](#)]
17. Jones, J.B.; Segnit, E.R. The nature of opal I. Nomenclature and constituent Phases. *J. Geol. Soc. Aust.* **1971**, *18*, 57–68. [[CrossRef](#)]
18. Jones, J.B.; Segnit, E.R. Nomenclature and structure of natural disordered (opaline) silica. A comment on the paper “A new interpretation of the structure of disordered  $\alpha$ -cristobalite” by M.J. Wilson, J.D. Russell and J.M. Tait. *Contrib. Mineral. Petrol.* **1975**, *51*, 231–234. [[CrossRef](#)]
19. Smith, D.K. Opal, cristobalite, and tridymite: Noncrystallinity versus crystallinity, nomenclature of the silica minerals and bibliography. *Powder Diffr.* **1998**, *13*, 2–19. [[CrossRef](#)]
20. Curtis, N.J.; Gascooke, J.R.; Johnston, M.R.; Pring, A. A review of the classification of opal with reference to recent new localities. *Minerals* **2019**, *9*, 299. [[CrossRef](#)]
21. Iler, R.K. *The Chemistry of Silica*; John Wiley & Sons: New York, NY, USA, 1978; p. 896, ISBN 978-0-471-02404-0.
22. Pecover, S.R. A new genetic model for the origin of opal in the Great Australian Basin. Mesozoic Geology of the Eastern Australia Plate Conference, Geological Society of Australia. *Ext. Abstr.* **1996**, *43*, 450–454.
23. Pecover, S.R. The new syntectonic model of origin to explain the formation of opal veins (“seams” and “nobbies”), breccia pipes (“blows”) and faults (“slides”) at Lightning Ridge. In Proceedings of the 1st National Opal Symposium, Lightning Ridge, Australia; 1999; pp. 1–31.
24. Pecover, S.R. Structures related to opal deposits at Lightning Ridge. Symposium: Exploring for opal. In *The Earth Resources Foundation and the Lightning Ridge Miners Association*; The University of Sydney: Camperdown, Australia, 2003; pp. 1–5.
25. Pecover, S. Breccia Pipes: Fluid Pathways of the Opal Gods. 4th National Opal Symposium, Lighting Ridge. 2005. Available online: [https://www.researchgate.net/publication/319255338\\_BRECCIA\\_PIPES\\_-\\_FLUID\\_PATHWAYS\\_OF\\_THE\\_OPAL\\_GODS](https://www.researchgate.net/publication/319255338_BRECCIA_PIPES_-_FLUID_PATHWAYS_OF_THE_OPAL_GODS) (accessed on 25 August 2023).
26. Pecover, S. Australian opal resources: Outback spectral fire. *Rocks Miner.* **2007**, *82*, 103–115. [[CrossRef](#)]
27. Pecover, S. *Recent Advances to the Syntectonic Model and Its Applicability to Opal Exploration Along the Collarenebri Antiform*; Pan Gem Resources (Aust) Ltd. 2011, pp. 1–23. Available online: <https://vdocuments.net/recent-advances-to-the-syntectonic-model-and-its-applicability-to-opal-exploration-along-the-collarenebri-antiform-full-paper-figures.html?page=1> (accessed on 25 August 2023).
28. Pecover, S. Key Features of Opal Vein Deposits at Lightning Ridge, NSW, Australia, 34 International Geological Conference, Australia 2012, Sydney, Australia. Available online: [https://www.researchgate.net/publication/319255402\\_KEY\\_FEATURES\\_OF\\_OPAL\\_Vein\\_DEPOSITS\\_AT\\_LIGHTNING RIDGE\\_NSW\\_AUSTRALIA\\_Pan\\_Gem\\_Resources\\_Aust\\_Pty\\_Ltd\\_Photo\\_by\\_Sarah\\_Pecover/link/599e373d0f7e9b892bb40f13/download](https://www.researchgate.net/publication/319255402_KEY_FEATURES_OF_OPAL_Vein_DEPOSITS_AT_LIGHTNING RIDGE_NSW_AUSTRALIA_Pan_Gem_Resources_Aust_Pty_Ltd_Photo_by_Sarah_Pecover/link/599e373d0f7e9b892bb40f13/download) (accessed on 7 July 2023).
29. Pecover, S. Australian Opal- How Did It Form? *Teacher Earth Science Education Program Case Study 1.006*. 2015. Available online: [https://www.researchgate.net/publication/319235421\\_Australian\\_Opal-How\\_did\\_it\\_form](https://www.researchgate.net/publication/319235421_Australian_Opal-How_did_it_form) (accessed on 25 August 2023).
30. Behr, H.J.; Behr, K.; Watkins, J.J. Cretaceous microbes—Producer of black opal at Lightning Ridge, NSW, Australia. In Proceedings of the 15th Australian Geological Convention, Society of Australia Abstracts, Sydney, Australia, 3–7 July 2000; Volume 59, p. 28.
31. Watkins, J.J.; Behr, H.J.; Behr, K. Fossil microbes in opal from Lightning Ridge—Implications for the formation of opal. *Q. Notes Geol. Surv. New South Wales* **2011**, *136*, 1–21.
32. Gallacher, A.D. Geochemistry of Sedimentary Opal, Hebel, Southern Queensland, Chapter 6. Biominerization, the Possible Role of Microbes in the Redistribution of Silica; Weathering and Genesis of Opal. Ph.D. Thesis, School of Earth Sciences, The University of Melbourne, Melbourne, Australia, 2001; pp. 138–146.

33. Herrmann, J.R.; Maas, R.; Rey, P.F.; Best, S.P. The nature and origin of pigments in black opal from Lightning Ridge, New South Wales, Australia. *Aust. J. Earth Sci.* **2019**, *66*, 1027–1039. [CrossRef]
34. Dowell, K.; Mavrogenes, J.; McPhail, D.C.; Watkins, J. Origin and timing of formation of precious black opal nobbies at Lightning Ridge. In *Regolith and Landscape of Eastern Australia*; Roach, I.C., Ed.; CRC LEME: Sydney, Australia, 2002; pp. 18–20.
35. Deveson, B. Microbes Associated with Precious Opal and the Implications for the Age of the Opal: Research Note. 2022. Available online: [https://www.researchgate.net/publication/358794316\\_Microbes\\_associated\\_with\\_precious\\_opal\\_and\\_the\\_implications\\_for\\_the\\_age\\_of\\_the\\_opal\\_Research\\_note](https://www.researchgate.net/publication/358794316_Microbes_associated_with_precious_opal_and_the_implications_for_the_age_of_the_opal_Research_note) (accessed on 25 August 2023).
36. Deveson, B. The Role of Artesian Water in the Formation of Precious Opal. Presented at 2007, Opal Symposium Coober Pedy. Available online: [https://www.researchgate.net/publication/338828655\\_The\\_role\\_of\\_artesian\\_water\\_in\\_theFormation\\_of\\_precious\\_opal\\_in\\_the\\_Lightning\\_Ridge\\_district](https://www.researchgate.net/publication/338828655_The_role_of_artesian_water_in_theFormation_of_precious_opal_in_the_Lightning_Ridge_district) (accessed on 25 August 2023).
37. Deveson, B. A New Model of the Formation of Precious Opal: Updated Notes, April 2022. Available online: [https://www.researchgate.net/publication/360235468\\_Opal\\_New\\_Model\\_updated\\_notes](https://www.researchgate.net/publication/360235468_Opal_New_Model_updated_notes) (accessed on 25 August 2023).
38. Deveson, B. The origin of precious opal. *Aust. Gemmol.* **2004**, *22*, 50–58.
39. Dickson, B.L. Which water formed Australian sediment-hosted precious and potch opal? *Aust. J. Earth Sci.* **2019**, *66*, 644–655. [CrossRef]
40. Senior, B.R.; Chadderton, L.T. Natural gamma radioactivity and exploration for precious opal in Australia. *Aust. Gemmol.* **2007**, *23*, 160–176.
41. Smallwood, A. 35 years on. A new look at synthetic opal. *Aust. Gemmol.* **2003**, *21*, 438–447.
42. Hodges, M.A. Len Cram An Opal Icon. Available online: <https://www.sunriseopals.com/pages/len-cram-an-opal-icon> (accessed on 12 July 2023).
43. McManus, G. The man who grows opals. *Australas. Post* **1988**, *6*, 18–20.
44. Shepherd, R. *The Birth of Opal—Natural and Synthetic*; CreateSpace Independent Publishing: Scotts Valley, CA, USA, 2013; p. 460.
45. Solingen, A.A. Growing opals—Australian style. *Creation* **1989**, *12*, 10–15.
46. Stelling, A.A. Rapid opals in the Outback. *Answ. Mag.* **2015**, *20*, 46–48.
47. Hounslow, M.H. Significance of localized pore pressures to the genesis of septarian concretions. *Sedimentology* **1997**, *44*, 1133–1147. [CrossRef]
48. Pratt, B.R. Septarian concretions: Internal cracking caused by synsedimentary earthquakes. *Sedimentology* **2001**, *48*, 189–213. [CrossRef]
49. Burt, F.A. Melikaria: Vein complexes resembling septaria veins in form. *J. Geol.* **1928**, *6*, 544–549. [CrossRef]
50. Woodward, A.S. On remains of a megalosaurian dinosaur from New South Wales. *Rep. Br. Assoc. Adv. Sci.* **1910**, *79*, 482–483.
51. von Huene, F. Die fossile Reptil-Ordnung Saurischia, ihre Entwicklung und Geschichte. *Monogr. Geol. Und. Palaeontol.* **1932**, *1*, 361.
52. Bell, P.R.; Herne, M.C.; Brougham, T.; Smith, E.T. Ornithopod diversity in the Griman Creek Formation (Cenomanian), New South Wales, Australia. *PeerJ* **2018**, *6*, e6008. [CrossRef] [PubMed]
53. Bell, P.R.; Cau, A.; Fanti, F.; Smith, E. A large-clawed theropod (Dinosauria: Tetanurae) from the Lower Cretaceous of Australia and the Gondwanan origin of megaraptorid theropods. *Gondwana Res.* **2016**, *36*, 473–487. [CrossRef]
54. Brougham, T.; Smith, E.T.; Bell, P.R. Noasaurids are a component of the Australian ‘mid’-Cretaceous theropod fauna. *Sci. Rep.* **2020**, *10*, 1428. [CrossRef] [PubMed]
55. Frauenfelder, T.; Bell, P.R.; Campione, N.E.; Smith, E.T. Diversity and paleoecology of Australia’s southern-most sauropods, Griman Creek Formation (Cenomanian) New South Wales. *Lethaia* **2021**, *54*, 354–367. [CrossRef]
56. Archer, M.; Flannery, T.F.; Ritchie, A.; Molnar, R.E. First Mesozoic mammal from Australia—An early Cretaceous monotreme. *Nature* **1985**, *318*, 363–366. [CrossRef]
57. Flannery, T.F.; Archer, M.; Rich, T.H.; Jones, R. A new family of monotremes from the Cretaceous of Australia. *Nature* **1995**, *377*, 418–420. [CrossRef]
58. Mustoe, G.E. Non-mineralized fossil wood. *Geosciences* **2018**, *8*, 223. [CrossRef]
59. Lucjaz, J.A.; Leavitt, S.W.; Csank, A.Z.; Panyushkina, I.P. Comment on “non mineralized fossil wood” by George E. Mustoe (Geosciences, 2018). *Geosciences* **2018**, *8*, 462.
60. Mustoe, G.E. Wood petrification: A new view of permineralization and replacement. *Geosciences* **2017**, *7*, 119. [CrossRef]
61. Berkshire Community College Bioscience Library. A Public Domain Open Educational Resource. Berkshire County, MA, USA. Available online: <https://blogs.berkshirecc.edu/bccoer/plant-morphology-angiosperm-stems/> (accessed on 25 August 2023).
62. Bell, P.R.; Bicknell, R.D.C.; Smith, E.T. Crayfish bio-gastroliths from eastern Australia and the middle Cretaceous distribution of Parastacidae. *Geol. Mag.* **2020**, *57*, 1023–1030. [CrossRef]
63. Utami, W.S.; Herdianita, N.R.; Atmaja, R.W. The Effect of Temperature and pH on the Formation of Silica Scaling of Dieng Geothermal Field, Central Java, Indonesia. In Proceedings of the Thirty-Ninth Workshop on Geothermal Reservoir Engineering, Stanford University, Stanford, CA, USA, 24–26 February 2014.
64. Nicholson, K. *Geothermal Fluids: Chemistry and Exploration Techniques*; Springer: Berlin/Heidelberg, Germany, 1968; 263p.
65. Pewkiang, B.; Pring, A.; Brugger, J. Opalisation of fossil bone and wood: Clues to the formation of precious opal. In *Regolith*; Roach, I.C., Ed.; CR LME: Sydney, Australia, 2004; pp. 264–268.
66. Pewkiang, B.; Pring, A.; Brugger, J. The formation of precious opal: Clues from the opalisation of bone. *Can. Mineral.* **2008**, *46*, 139–149. [CrossRef]

67. Wedel, M.J. The evolution of vertebral pneumaticity in sauropod dinosaurs. *J. Vert. Paleontol.* **2003**, *23*, 344–357. [CrossRef]
68. Aureliano, T.; Ghilardi, A.M.; Müller, R.T.; Kerber, L.; Pretto, F.; Fernandez, M.A.; Ricard-Btanco, F.; Wedel, M. The absence of an invasive air sac system in the earliest dinosaurs suggests multiple origins of vertebral pneumaticity. *Sci. Rep.* **2022**, *12*, 20844. [CrossRef] [PubMed]
69. Gianchinia, F.A.; Zurriaguzm, V.L. Vertebral pneumaticity of the paravian theropod *Unerlagiacomanhuensis*, from the Upper Cretaceous of Patagonia, Argentina. *Cretac. Res.* **2021**, *127*, 104925. [CrossRef]
70. Taylor, M.P.; Wedel, M.J. Why Is Vertebral Pneumaticity in Sauropod Dinosaurs so Variable? *Quios* 2021. Available online: <https://www.qeios.com/read/1G6J3Q.5> (accessed on 15 September 2023).
71. Brougham, T.; Smith, E.T.; Bell, P.R. New theropod (Tetanurae: Avetheropoda) material from the ‘mid’-Cretaceous Griman Creek Formation at Lightning Ridge, New South Wales, Australia. *R. Soc. Open Sci.* **2018**, *6*, 180826. [CrossRef] [PubMed]
72. Hunt, A.P.; Lucas, S.G. Descriptive terminology of coprolites and recent feces. In *Vertebrate Coprolites*; Hunt, A.P., Milà, J., Lucas, S.G., Spielmann, J.A., Eds.; New Mexico Museum of Natural History and Science, Bull: Albuquerque, NM, USA, 2012; pp. 152–160.
73. Mustoe, G.E. Silicification of wood: An overview. *Minerals* **2023**, *13*, 206. [CrossRef]
74. Palgutová, S.; Štrba, L’. Geoheritage of the precious opal bearing zone in Libanka Mining District (Slovakia) and its geotourism and geoeducation potential. *Land* **2022**, *11*, 2293. [CrossRef]
75. Miró, J.; Martin-Martin, J.D.; Ibáñez, J.; Anadón, P.; Oms, O.; Tritila, J.; Caja, M.A. Opaline chert nodules in maar lake sediments from Camp del Ninots (La Selva basin, NE Spain). *Geo-Temas* **2016**, *16*, 387–390.
76. Damour, A. Chemical composition of menilite. *Z. Fuer Krist. Und. Mineral.* **1888**, *11*, 640–641.
77. Porfiriev, V. Carpathian menilite. *Rocks Miner.* **1970**, *45*, 145–146.
78. Mustoe, G.E. Late Tertiary petrified wood from Nevada, USA: Evidence of multiple silicification processes. *Geosciences* **2015**, *5*, 286–309. [CrossRef]
79. Chauviré, B.; Mollé, V.; Guichard, F.; Rondeau, B.; Thomas, P.S. Cracking in gem opals. *Minerals* **2023**, *13*, 356. [CrossRef]
80. Smallwood, A.G.; Thomas, P.; Ray, A.S. Comparative analysis of sedimentary and volcanic precious opals from Australia. *J. Australas. Ceram. Soc.* **2008**, *44*, 17–22.
81. Liesegang, M.; Tomaschek, F. Tracing the continental diagenetic loop of the opal-A to opal-CT transition with X-ray diffraction. *Sed. Geol.* **2020**, *398*, 105603. [CrossRef]
82. Murata, K.J.; Nakata, J.K. Cristobalitic Stage in the Diagenesis of Diatomaceous Shale. *Science* **1974**, *184*, 567–568. [CrossRef]
83. Ijima, A.; Tada, R. Silica diagenesis of Neogene diatomaceous and volcanioclastic sediments in northern Japan. *Sedimentology* **1981**, *28*, 185–200. [CrossRef]
84. Mizutani, S. Silica Minerals in the Early Stage of Diagenesis. *Sedimentology* **1970**, *15*, 419–436. [CrossRef]
85. Mizutani, S. Progressive ordering of cristobalite in early stages of diagenesis. *Contrib. Mineral. Petrol.* **1977**, *129*, 129–140. [CrossRef]
86. Hein, J.R.; Scholl, D.W.; Barron, J.A.; Jones, M.G.; Miller, J. Diagenesis of late Cenozoic diatomaceous deposits and formation of the bottom simulating reflector in the southern Bering Sea. *Sedimentology* **1978**, *25*, 155–181. [CrossRef]
87. Hein, J.R.; Yeh, H.W.; Barron, J.A. Eocene Diatom Chert from Adak Island, Alaska. *J. Sediment. Res.* **1990**, *60*, 250–257. [CrossRef]
88. Mustoe, G.E. Diatomaceous origin of siliceous shale in Eocene lake beds of central British Columbia. *Can. J. Earth Sci.* **2005**, *42*, 231–241. [CrossRef]
89. Cady, S.L.; Wenk, H.R.; Downing, K.H. HRTEM of microcrystalline opal in chert and porcellanite from the Monterey Formation, California. *Am. Mineral.* **1996**, *81*, 1380–1395. [CrossRef]
90. Kastner, M.; Keene, J.; Gieskes, J. Diagenesis of siliceous oozes—I. Chemical controls on the rate of opal-A to opal-CT transformation—An experimental study. *Geochim. Cosmochim. Acta* **1977**, *41*, 1041–1059. [CrossRef]
91. Ernst, W.G.; Calvert, S.E. An experimental study of the recrystallization of porcellanite and its bearing on the origin of some bedded cherts. *Am. J. Sci.* **1969**, *267-A*, 114–133. ISSN/ISBN 0002-9599.
92. Behl, R.J.; Moores, E.M.; Sloan, D.; Stout, D.L. Since Bramlette (1946): The Miocene Monterey Formation of California revisited. In *Classic Cordilleran Concepts: A View from California*; Geological Society of America: Boulder, CO, USA, 1999; pp. 301–313.
93. Hesse, R. Diagenesis #13. Origin of chert: Diagenesis of biogenic siliceous sediments. *Geosci. Can.* **1988**, *15*, 171–192.
94. Herdianita, N.R.; Browne, P.R.L.; Rodgers, K.A.; Campbell, K.A. Mineralogical and morphological changes accompanying aging of siliceous sinter. *Miner. Depos.* **2000**, *7*, 232–242. [CrossRef]
95. Lynne, B.Y.; Campbell, K.A.; Moore, J.N.; Browne, P.R.L. Diagenesis of 1900-year-old siliceous sinter (opal-A to quartz) at Opal Mound, Roosevelt Hot Springs, Utah, USA. *Sed. Geol.* **2005**, *179*, 249–278. [CrossRef]
96. Williams, L.A.; Parks, G.A.; Crerar, D.A.; Silica Diagenesis, I. Solubility Controls. *J. Sediment. Res.* **1985**, *55*, 301–311. [CrossRef]
97. Mattheney, L.P.; Knauth, L.P. New isotopic temperature estimates for early silica diagenesis in bedded cherts. *Geology* **1993**, *21*, 519–522. [CrossRef]
98. Kastner, M.; Gieskes, J.M. Opal-A to opal-CT transformation. A kinetic study. *Dev. Sedimentol.* **1983**, *25*, 211–227.
99. Chen, T.; Xu, H.; Xu, X.; Yue, S. Oscillation of opal-A and opal-CT layers as indicators of paleoclimate and paleohydrology changes. *Geol. Soc. Am. Annu. Meet. Denver USA Abstr. Programs* **2002**, *34*, 383.
100. Hoffmann, T.D.; Reeksting, B.J.; Gebhard, S. Bacteria-induced mineral precipitation: A mechanistic review. *Microbiology* **2021**, *167*, 001049. [CrossRef] [PubMed]

101. Smith, B.Y.; Turner, S.J.; Rodgers, K.A. Opal-A and associated microbes from Warakei, New Zealand: The first 300 days. *Mineral. Mag.* **2003**, *67*, 563–569. [[CrossRef](#)]
102. Farfan, G.A.; McKeown, D.A.; Post, J.E. Mineralogical characterization of biosilicas versus geological analogs. *Geobiology* **2023**, *21*, 520–533. [[CrossRef](#)] [[PubMed](#)]
103. Horton, D. Australian sedimentary opal—Why is Australia unique? *Aust. Gemmol.* **2002**, *21*, 287–294.

**Disclaimer/Publisher’s Note:** The statements, opinions and data contained in all publications are solely those of the individual author(s) and contributor(s) and not of MDPI and/or the editor(s). MDPI and/or the editor(s) disclaim responsibility for any injury to people or property resulting from any ideas, methods, instructions or products referred to in the content.